[3] M. Huang, J.M. Orenstein, M.A. Martin, E.O. Freed, p6Gag is required for particle production from full-length human immunodeficiency virus type 1 molecular clones expressing protease, J. Virol. 69 (1995) 6810–6818.

[4] O. Pornillos, J.E. Garrus, W.I. Sundquist, Mechanisms of enveloped RNA virus budding, Trends Cell Biol. 12 (2002) 569–579.

[5] V.M. Vogt, Ubiquitin in retrovirus assembly: actor or bystander? Proc. Natl. Acad. Sci. USA 97 (2000) 12945–12947.

[6] A. Patnaik, J.W. Wills, In vivo interference of Rous sarcoma virus budding by cis expression of a WW domain, J. Virol. 76 (2002) 2789–2795.

[7] B. Strack, A. Calistri, M.A. Accola, G. Palu, H.G. Gottlinger, A role for ubiquitin ligase recruitment in retrovirus release, Proc. Natl. Acad. Sci. USA 97 (2000) 13063–13068.

[8] J. Yasuda, E. Hunter, A proline-rich motif (PPPY) in the Gag polyprotein of Mason–Pfizer monkey virus plays a maturation-independent role in virion release, J. Virol. 72 (1998) 4095–4103.

[9] J. Martin-Serrano, T. Zang, P.D. Bieniasz, HIV-1 and Ebola virus encode small peptide motifs that recruit Tsg101 to sites of particle assembly to facilitate egress, Nat. Med. 7 (2001) 1313–1319.

[10] E.L. Myers, J.F. Allen, Tsg101, an inactive homologue of ubiquitin ligase e2, interacts specifically with human immunodeficiency virus type 2 gag polyprotein and results in increased levels of ubiquitinated gag, J. Virol. 76 (2002) 11226–11235.

[11] L.J. Parent, R.P. Bennett, R.C. Craven, T.D. Nelle, N.K. Krishna, J.B. Bowzard, C.B. Wilson, B.A. Puffer, R.C. Montelaro, J.W. Wills, Positionally independent and exchangeable late budding functions of the Rous sarcoma virus and human immunodeficiency virus Gag proteins, J. Virol. 69 (1995) 5455–5460.

[12] B. Yuan, S. Campbell, E. Bacharach, A. Rein, S.P. Goff, Infectivity of Moloney murine leukemia virus defective in late assembly events is restored by late assembly domains of other retroviruses, J. Virol. 74 (2000) 7250–7260.

[13] R.N. Harty, M.E. Brown, G. Wang, J. Huibregtse, F.P. Hayes, A PPxY motif within the VP40 protein of Ebola virus interacts physically and functionally with a ubiquitin ligase: implications for filovirus budding, Proc. Natl. Acad. Sci. USA 97 (2000) 13871–13876.

[14] J.M. Licata, M. Simpson-Holley, N.T. Wright, Z. Han, J. Paragas, R.N. Harty, Overlapping motifs (PTAP and PPEY) within the Ebola virus VP40 protein function independently as late budding domains: involvement of host proteins TSG101 and VPS-4, J. Virol. 77 (2003) 1812–1819.

[15] R.N. Harty, J. Paragas, M. Sudol, P. Palese, A proline-rich motif within the matrix protein of vesicular stomatitis virus and rabies virus interacts with WW domains of cellular proteins: implications for viral budding, J. Virol. 73 (1999) 2921–2929.

[16] A. Kikonyogo, F. Bouamr, M.L. Vana, Y. Xiang, A. Aiyar, C. Carter, J. Leis, Proteins related to the Nedd4 family of ubiquitin protein ligases interact with the L domain of Rous sarcoma virus and are required for gag budding from cells, Proc. Natl. Acad. Sci. USA 98 (2001) 11199–11204.

[17] J. Yasuda, E. Hunter, M. Nakao, H. Shida, Functional involvement of a novel Nedd4-like ubiquitin ligase on retrovirus budding, EMBO Rep. 3 (2002) 636–640.

[18] O. Pornillos, S.L. Alam, D.R. Davis, W.I. Sundquist, Structure of the Tsg101 UEV domain in complex with the PTAP motif of the HIV-1 p6 protein, Nat. Struct. Biol. 9 (2002) 812–817.

[19] L. VerPlank, F. Bouamr, T.J. LaGrassa, B. Agresta, A. Kikonyogo, J. Leis, C.A. Carter, Tsg101, a homologue of ubiquitin-conjugating (E2) enzymes, binds the L domain in HIV type 1 Pr55(Gag), Proc. Natl. Acad. Sci. USA 98 (2001) 7724–7729.

[20] D.G. Demirov, A. Ono, J.M. Orenstein, E.O. Freed, Overexpression of the N-terminal domain of TSG101 inhibits HIV-1 budding by blocking late domain function, Proc. Natl. Acad. Sci. USA 99 (2002) 955–960.

[21] J.E. Garrus, U.K. von Schwedler, O.W. Pornillos, S.G. Morham, K.H. Zavitz, H.E. Wang, D.A. Wettstein, K.M. Stray, M. Cote, R.L. Rich, D.G. Myszka, W.I. Sundquist, Tsg101 and the vacuolar protein sorting pathway are essential for HIV-1 budding, Cell 107 (2001) 55–65.

[22] I. Le Blanc, A.R. Rosenberg, M.C. Dokhelar, Multiple functions for the basic amino acids of the human T-cell leukemia virus type 1 matrix protein in viral transmission, J. Virol. 73 (1999) 1860–1867.

[23] H. Wang, K.M. Norris, L.M. Mansky, Analysis of bovine leukemia virus gag membrane targeting and late domain function, J. Virol. 76 (2002) 8485–8493.

[24] J. Yasuda, M. Nakao, Y. Kawaoka, H. Shida, Nedd4 regulates egress of Ebola virus-like particles from host cells, J. Virol. 77 (2003) 9987–9992.

[25] Y. Tanaka, B. Lee, T. Inoi, H. Tozawa, N. Yamamoto, Y. Hinuma, Antigens related to three core proteins of HTLV-I (p24, p19 and p15) and their intracellular localizations, as defined by monoclonal antibodies, Int. J. Cancer 37 (1986) 35–42.

[26] I. Le Blanc, M.C. Prevost, M.C. Dokhelar, A.R. Rosenberg, The PPPY motif of human T-cell leukemia virus type 1 Gag protein is required early in the budding process, J. Virol. 76 (2002) 10024–10029.

[27] L. Garnier, J.W. Wills, M.F. Verderame, M. Sudol, WW domains and retrovirus budding, Nature 381 (1996) 744–745.

[28] T. Anan, Y. Nagata, H. Koga, Y. Honda, N. Yabuki, C. Miyamoto, A. Kuwano, I. Matsuda, F. Endo, H. Saya, M. Nakao, Human ubiquitin-protein ligase Nedd4: expression, subcellular localization and selective interaction with ubiquitin-conjugating enzymes, Genes Cells 3 (1998) 751–763.

[29] R. Goila-Gaur, D.G. Demirov, J.M. Orenstein, A. Ono, E.O. Freed, Defects in human immunodeficiency virus budding and endosomal sorting induced by TSG101 overexpression, J. Virol. 77 (2003) 6507–6519.

bait4/zpq-pnas/zpq-pnas/zpq-orig/zpq7687d05g | flemingj | S=5 | 2/15/05 | 13:34 | 4/Color Figure(s): 1 | Art: 04-06671 | Input-llt

Genetically stable and fully effective smallpox vaccine strain constructed from highly attenuated vaccinia LC16m8

Minoru Kidokoro*†, Masato Tashiro*, and Hisatoshi Shida‡

*Department of Virology III, National Institute of Infectious Diseases, 4-7-1 Gakuen, Musashimurayama, Tokyo 208-0011, Japan; and ‡Institute for Genetic Medicine, Hokkaido University, Kita-15, Nishi-7, Kita-ku, Sapporo, Hokkaido 060-0815, Japan

Edited by Peter Palese, Mount Sinai School of Medicine, New York, NY, and approved February 3, 2005 (received for review September 9, 2004)

A highly attenuated LC16m8 (m8) smallpox vaccine has been licensed in Japan because of its extremely low neurovirulence profile, which is comparable to that of replication incompetent strains of vaccinia virus. From 1973 to 1975, m8 was administrated to >100,000 infants where it induced levels of immunity similar to that of the originating Lister strain, without any serious side effects. Recently, we observed that m8 reverts spontaneously to large plaque forming clones that possess virulence equivalent to that of LC16mO, a parental virus strain of m8. Here, we report that the *B5R* gene is responsible for the reversion, and that we could construct a more genetically stable virus by deleting *B5R* from m8. The protective immunogenicity of the vaccine proved to be equivalent to that of the U.S.-licensed product Dryvax, and much superior to modified vaccinia Ankara in a mouse model. Furthermore, the vaccine strain never elicited any symptoms in severe combined immunodeficiency disease mice, even at a dose 1,000-fold greater than that used in the immune protection experiments, which is in contrast to the lethal pathogenicity induced by Dryvax inoculation of severe combined immunodeficiency disease mice. Our results suggest that this vaccine strain is a good candidate as a suitable smallpox vaccine and a vector virus, and that B5R is not essential for protective immunity against smallpox.

B5R gene | reversion

Although smallpox was eradicated >20 years ago (1), the necessity of a smallpox vaccine has been reawakened by concerns of bioterrorism using the smallpox virus (2) and outbreaks of monkeypox (3). However, the current vaccine in the United States, Dryvax, occasionally elicits serious adverse effects, including postvaccinal encephalitis (4). Accordingly, a safer smallpox vaccine is much needed.

In Japan, a highly attenuated form of vaccine referred to as LC16m8 (m8) was administrated to >100,000 infants without any serious adverse events, and proved to be as immunogenic as the Lister (LO) strain (5, 6), a once widely used vaccine. m8 was indirectly isolated from LO through intermediate strains, such as LC16mO (mO) and LC16. m8, a variant that forms small-sized pocks, is a direct descendant of mO, which itself is a clone that forms medium-sized pocks, isolated from the LC16 strain (5). LC16 was selected from LO based on its temperature sensitivity (5, 7, 8). In rabbit and monkey models, the neurovirulence of m8 was markedly reduced in comparison with other vaccine strains (5, 7–9), including LO and Dryvax (10, 11), and comparable to the replication-defective mutant DIs (12). Moreover, m8 exhibited a markedly diminished dermal reaction in both rabbits and humans and a lower fever ratio compared with mO in clinical trials (5, 6). Therefore, m8 was finally adopted as a vaccine strain instead of mO (6).

Takahashi-Nishimaki *et al.* (13) first identified the vaccinia virus (VV) gene *B5R* as responsible for large plaque formation and proliferating ability in Vero cells. m8 has lost the *B5R* function as the result of a frameshift mutation brought about by a single base deletion in the ORF. *B5R* encodes a 42-kDa glycoprotein that is involved in packaging the intracellular matured virion with trans-Golgi membrane or endosomal cisternae to form an intracellular enveloped virion (IEV) (14–16). IEV is transported along microtubules to the cell periphery (17, 18) where it adheres to the cell surface as a cell-associated enveloped virion (CEV). B5R, in cooperation with the A36R and A33R proteins, also participates in the Src kinase-dependent process of forming of actin-containing microvilli and releasing CEV from the cell surface to form an extracellular enveloped virion (EEV) (19, 20). Despite its relative paucity of whole progeny virions, EEV plays an important role in dissemination within the host (21). Because anti-B5R antibodies can neutralize EEV, expression of *B5R* has been proposed as an effective smallpox vaccine (14, 22–25). In contrast, the results of the field trial in Japan showed that neutralization antibody titers induced by m8 were similar to a conventional LO vaccine (5, 6).

Recently, we found that m8 reverted spontaneously to large plaque-forming clones (LPCs).[§] The content of LPCs seemed to increase rapidly in proportion to passage number of the virus. Because LPCs emerged from plaque-purified m8, their generation appears to be an intrinsic property of m8. We were concerned that LPC contamination might ruin the safety of the m8 vaccine. Therefore, to improve the m8 strain, we tested whether *B5R* was the gene responsible for the reversion, because this gene has been correlated with large plaque formation. We then constructed genetically more stable virus by deleting *B5R*. Moreover, by using this virus, we were able to evaluate the contribution of *B5R* to protective immunity against smallpox.

Methods

Virus Preparations. m8 was obtained from Chiba Serum Institute (Chiba, Japan). m8rc (plaque-purified m8 to minimize contamination by revertants) and the revertant viruses (LPCs) were isolated from the m8 stock by three serial plaque purifications in RK13 cells. The modified VV Ankara (MVA) (26, 27) and Western Reserve (WR) viruses were obtained from S. Morikawa (National Institute of Infectious Diseases, Tokyo). MVA was propagated and titrated in chicken embryo fibroblasts. Other viruses were propagated and titrated in RK13 cells, and purified by sedimentation through a 36% sucrose cushion. A vial of Dryvax vaccine, obtained from I. K. Damon and J. Becher (Centers for Disease Control and Prevention, Atlanta), was dissolved in the enclosed solvent, aliquoted, and stored at −80°C. Construction of m8B5R, which harbors the intact *B5R* gene,

This paper was submitted directly (Track II) to the PNAS office.

Abbreviations: m8, LC16m8; mO, LC16mO; LO, Lister; LPC, large plaque-forming clone; VV, vaccinia virus; MVA, modified VV Ankara; SCID, severe combined immunodeficiency disease; EEV, extracellular enveloped virion; PRK, primary rabbit kidney; pfu, plaque-forming units; RED_{50}, 50% rash expression dose; ERD_{50}, 50% erythema dose; WR, Western Reserve.

†To whom correspondence should be addressed. E-mail: kidokoro@nih.go.jp.

§Kidokoro, M., Eshita, K. & Horiuchi, K. Sixth Meeting of the Japanese Society for Vaccinology (in Japanese), ●●●2002, abstr. ●●●.

m8Δ, which lacks the entire *B5R* gene, and m8dTM, which expresses only the ectodomain of the B5R protein, and characterization of their properties, including the structures of *B5R* in the viruses used, are described in more detail (Table 1 and Fig. 5, which are published as supporting information on the PNAS web site).

AQ: I

Western Blotting. We performed immunoblotting by using an antiserum from rabbits that were immunized with baculovirus-expressed recombinant B5R protein. The anti-B5R sera were used at a dilution of 1:200, and detected with a horseradish peroxidase-labeled secondary antibody and an ECL Plus kit (Amersham Pharmacia Biosciences, Piscataway, NJ).

AQ: J

Evaluation of Genetic Stabilities of VVs. We passaged the VVs in primary rabbit kidney (PRK) cells that are used for vaccine production 7 times at 30°C or 34°C, then in Vero cells 2 times at 34°C to amplify LPCs, or 10 times in PRK at 30°C or 34°C. We estimated the fraction of LPCs as the ratio of plaque counts on Vero cells to those on RK13 cells.

Animals. SCID mice (female, 6 weeks old) and BALB/c mice (female, 6 weeks old) were purchased from Charles River Japan (Kanagawa, Japan). Female Japan white rabbits (16 weeks old) were obtained from Kitayama Labes (Nagano, Japan). All animal experiments were approved by the National Institute of Infectious Diseases Animal Experiment Committee and were performed in accordance with guidelines for animal experiments performed at the National Institute of Infectious Diseases.

Skin Reaction Test in Rabbits. We conducted a skin reaction test as described (10). Briefly, after inoculating tenfold serial dilutions of VVs intradermally on rabbit backs, the diameters of erythema were measured daily for 1 week. Two animals were used for each viral strain, and each rabbit received two injections of the serial dilution series of a virus. Erythemas over 10 mm in diameter was scored as positive. The time at which erythemas reached their peak was determined for each animal, and the 50% erythema dose (ErD_{50}) was calculated by the Behrens and Karber method (28).

SCID Mice Infection Test. To establish an index for pathogenicity of VV against SCID mice, we defined a 50% rash expression dose (RED_{50}), which indicates the virus dose needed to induce a rash in 50% of the animals. After inoculating tenfold serial dilutions [10^3 to 10^7 plaque-forming units (pfu)] of VVs i.p. into a series

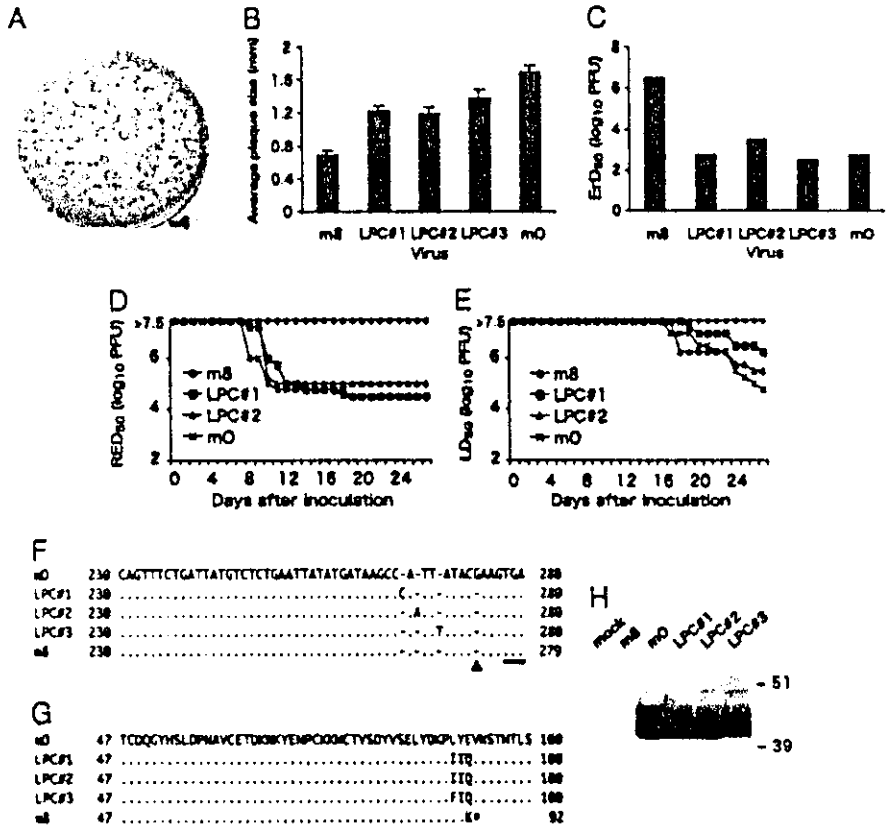

Fig. 1. Biological properties of LPC viruses. (*A*) The plaque configurations of LPCs contaminating an m8 virus stock. LPC viruses make considerably larger plaques than m8. (*B*) The mean plaque sizes of m8, mO, and plaque-purified LPCs. LPCs were isolated from an m8 vaccine stock solution. The data are presented as mean ± SD ($P < 0.05$). (*C*) The dermal reaction scores (ErD_{50}) of the LPCs intradermally inoculated in rabbits. (*D* and *E*) Pathogenicity of LPCs against SCID mice. The graphs show temporal changes of RED_{50} (*D*) and LD_{50} (*E*) for a 4-week period after inoculation. The m8 strain was asymptomatic even at the highest viral doses in this experiment (10^7 pfu). If all mice are killed by inoculation of 10^8 pfu of m8, its LD_{50} is $10^{7.5}$ pfu. Therefore, pathogenicity of asymptomatic group ought to be $> 10^{7.5}$ pfu. (*F* and *G*) Alignment of the *B5R* nucleotide sequences (*F*) and amino acid sequences (*G*) of mO, m8, and three LPC viruses. Numbers at both ends of the alignments indicate residue numbers. Dots, hyphens, and black triangles in the alignments show identical sequences, gaps, and the single-nucleotide deletion of m8, respectively. The bar and asterisk in the alignments indicate the termination codon. (*H*) Western blots of B5R in VV-infected RK13 cell-lysates. Duplex bands of B5R may be the result of differential glycosylation. Molecular weight markers are shown in kDa.

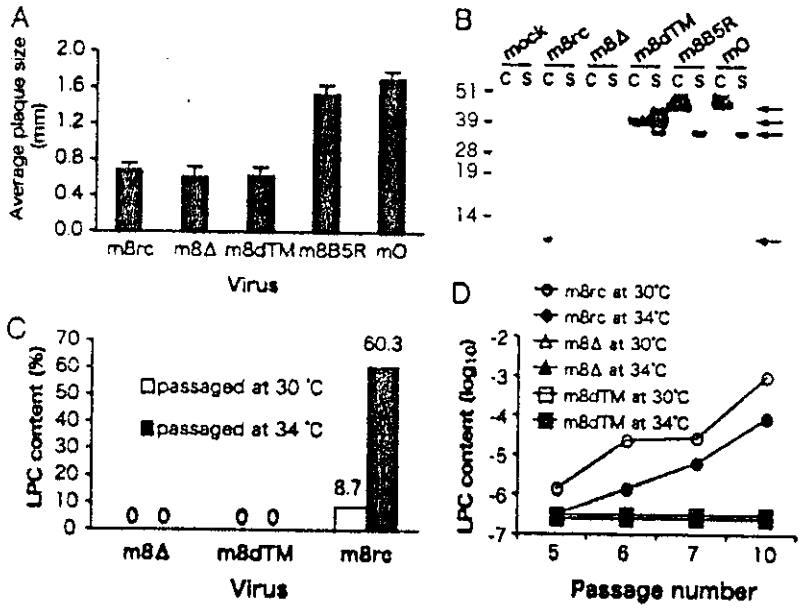

Fig. 2. Characterization of *B5R*-defective viruses (*A*) The average plaque sizes of m8rc-, m8Δ-, m8dTM-, and *B5R*-positive viruses (m8B5R and mO). The data are presented as mean ± SD. (*B*) Western blots of VV-infected RK13 cell lysates (lane C) and supernatants (lane S). m8rc expresses a short peptide (10 kDa) in the cell and supernatant lanes. The soluble ectodomain of B5R (38 kDa) is expressed from m8dTM. The smaller molecule (35 kDa) in the supernatant lanes of m8dTM, m8B5R, and mO is proteolytically cleaved B5R by cellular proteases. (*C* and *D*) Evaluation of genetic stability by serial passages in PRK and Vero cells under different temperatures (at 30°C or 34°C). The revertant contents of viruses that were passaged seven times in PRK cells and two times in Vero cells, are shown in *C*, and those contents passaged in PRK cells are shown in *D*.

of SCID mice, we calculated the viral doses required for inducing rash (RED_{50}) or killing (LD_{50}) in 50% of the animals by the Reed–Muench method, and followed both values for 4 weeks and 8 weeks.

BALB/c Protection Study. BALB/c mice (eight animals per group) were injected intramuscularly with a single dose of 10^4 to 10^6 pfu of VVs, bled at the tail artery 3 weeks later, and then challenged intranasally with 10^6 pfu of the WR strain 4 weeks after vaccination. Individual body weight was measured daily for 3 weeks, and animals with weight loss over 30% were killed.

Neutralization Assays. Serial fourfold dilutions (from 2^{-1} to 2^{-7}) of heat-inactivated mouse serum were mixed with solution containing ≈200 pfu of the WR strain, incubated for 16 h at 37°C, and inoculated on RK13 cells cultured in 48-well plates. Antibody titers were defined as the reciprocal of serum dilution that reduces viral plaques by 50%. All assays were performed in triplicate. The antibody titers of sera from a mock-immunized group were <2 in our assay system.

Statistical Methods. We used Microsoft EXCEL and ORIGIN (OriginLab, Northampton, MA) for statistical analysis. The differences in the mean plaque sizes and in body weight changes measured 5 days after viral challenge in the mouse model were determined by Student's *t* test, with $P < 0.05$ as the criterion for statistical significance. The results are summarized in Table 2, which is published as supporting information on the PNAS web site.

AQ: K

Results

F1

We isolated three LPC clones from m8 stock and compared several biomarkers with m8 and mO (Fig. 1). All of the clones exhibited phenotypical characteristics similar to mO, such as plaque size (Fig. 1*B*), dermal reactions in rabbits (ErD_{50}) (Fig. 1*C*), and pathogenicity to SCID mice (Fig. 1 *D* and *E*). Specifically, i.p. injection of 10^7 pfu of m8 elicited no overt symptoms over a 4-week period, whereas mO and two LPC clones induced a severe rash and then killed mice, even when administered at a dose (10^5 pfu) 100-fold lower than that of m8 (Fig. 1 *D* and *E*). The accelerated viral replication of LPCs in Vero cells (data not shown) also supported the similarity of the mO and LPC clones. Because the growth ability of mO has been linked to the *B5R* gene product, we hypothesized that the *B5R* gene might be involved in the reversion. Sequencing the LPC genomes revealed that the *B5R* ORF was restored in all of the LPCs, by a one-base insertion at sites just upstream of the deletion site in the m8 *B5R* (Fig. 1 *F* and *G*). Western blotting confirmed the expression of B5R proteins from these LPCs (Fig. 1*H*).

To prevent the reversion of the m8 *B5R* gene, we constructed *B5R* knockout viruses. First, we constructed a $B5R^+$ virus (named m8B5R) from m8 by introducing the complete *B5R* cloned from mO (Fig. 5 and Table 1). We then deleted the entire *B5R* sequence from m8B5R to construct m8Δ (Fig. 5 and Table 1). The resultant knockout virus formed plaques as small as the m8rc plaques that were then plaque-purified from m8 stock to minimize LPC contamination (Fig. 2*A*), and did not express the B5R protein in infected RK13 cells, whereas m8B5R and mO did (Fig. 2*B*). F2

One method by which to augment the immunogenicity of VV without increasing its pathogenicity may be the construction of VV that overexpresses a B5R derivative, which is fully immunogenic but loses its original function in the formation of EEV. The ectodomain of B5R has been reported to possess all epitopes necessary for induction of neutralizing antibody production (22, 29), whereas B5R must be anchored in the membrane for EEV formation (30). We constructed a VV (named m8dTM, Fig. 5 and Table 1) that expresses only the ectodomain of the B5R protein, by replacing the whole *B5R* region of m8B5R with the *B5R* ectodomain sequence placed downstream of the strong

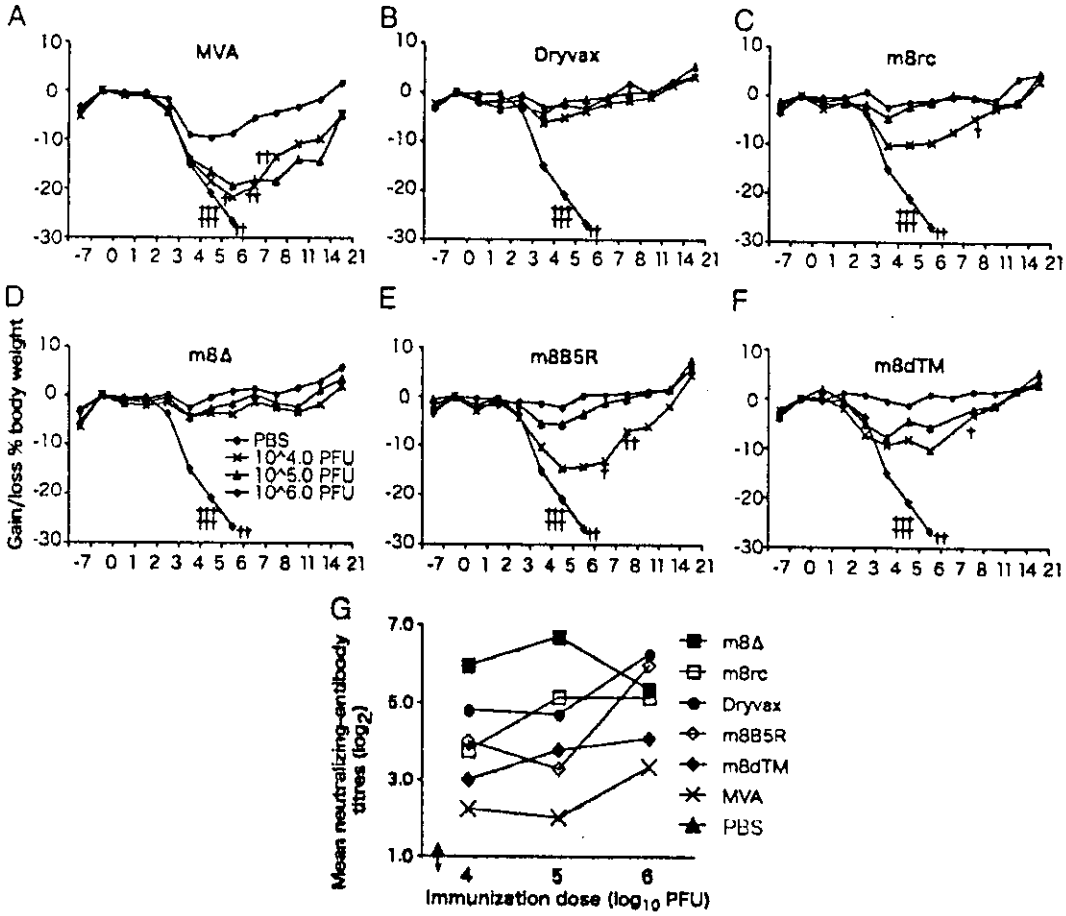

Fig. 3. Protective immunogenicity of vaccine candidate virus in mice. (*A–F*) Average body weight of mice immunized with $10^{4.0}$ to $10^{6.0}$ pfu of VVs intramuscularly and challenged intranasally with the WR strain. Cross marks indicate the mice that died or were killed because of 30% weight loss. (*G*) Average neutralizing antibody titers in mouse sera collected 3 weeks after immunization with VVs. The titers in sera from a Sham-immunized group were below the limit of detection.

promoter PSFJ1–10 (31), m8dTM also formed as small plaques as m8Δ, suggesting that this truncated B5R was not functional for EEV formation. As expected, m8dTM expresses a large quantity of a 38 kDa-truncated protein in the culture medium of infected cells (Fig. 2*B*).

To evaluate the genetic stability of the viruses and m8rc, we serially passaged the viruses in PRK cells and Vero cells. Under all conditions tested, including that for vaccine production (passage in PKR cells at 30°C), detectable levels (i.e., levels of $>10^{-6}$) of LPCs failed to emerge from either m8Δ or m8dTM, which is in contrast to the LPC generation from m8rc (Fig. 2 *C* and *D*). Each of the three viruses propagated at similar levels in the cultured cells. It should be noted that once LPCs appeared in the cultures, the fraction of LPCs derived from m8rc rapidly increased with the number of passages (Fig. 2*D*), suggesting it is of vital importance to prevent the emergence of LPCs for optimum quality control of the vaccine.

The protective immunogenicities of smallpox vaccine candidates were compared with other vaccine strains by using a mouse model challenged with a highly pathogenic VV, the WR strain (32) (Fig. 3 and Table 2). All mice immunized with doses of m8Δ or Dryvax survived, whereas all Sham-immunized mice, and 5/8, 3/8, 1/8 and 1/8 of mice immunized with 10^4 pfu of MVA, m8B5R, m8rc, or m8dTM, respectively, died or were killed because of a 30% weight loss (Fig. 3 *A–F*). At the lower doses, the mice immunized with m8Δ or Dryvax did not exhibit any significant differences in weight in a challenge after 5 days (*t* test, $P < 0.05$). Moreover, the m8Δ-immunized group lost less weight than the Dryvax-immunized group at the highest dose (Table 2). In contrast, the groups immunized with 10^4 pfu of m8rc, m8B5R, and all mice immunized with MVA, experienced a significant weight loss in comparison to m8Δ ($P < 0.05$, Table 2). The m8dTM-immunized group also showed significant weight loss by days 4 and 6 ($P = 0.012$ and 0.038, respectively, data not shown). Measurement of the neutralizing (NT) antibody titers elicited in the mice at 3 weeks after immunization (Fig. 3*G*) showed that m8Δ induced the highest titers among the viral strains at lower doses than the other immunizations. The next group, including Dryvax, m8rc, m8B5R, and m8dTM, induced NT antibodies with an efficiency intermediate between m8Δ and MVA. MVA was the least immunogenic virus: 10^6 pfu of MVA was required to induce significant NT antibodies.

The pathogenicity of the B5R-defective viruses was examined by ED_{50} in rabbits (Fig. 4*A*) and RED_{50} and LD_{50} in SCID mice (Fig. 4*B* and *C*). m8Δ and m8dTM exhibited an ED_{50} in rabbits similar to that of m8rc, whereas m8B5R induced the most severe dermal reaction among the strains examined (Fig. 4*A*). The pathogenicity of m8Δ and m8dTM to SCID mice was particularly

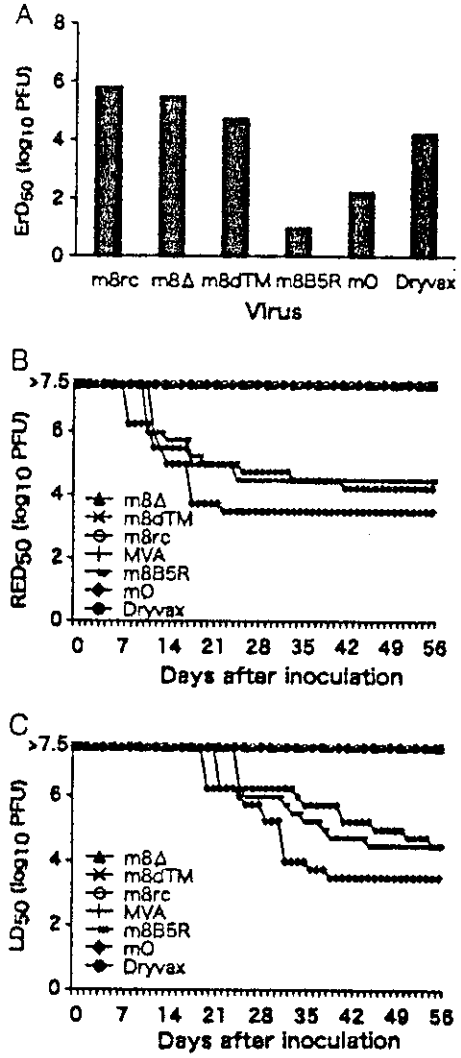

Fig. 4. Pathogenicity of vaccine candidate virus in animals. (*A*) The dermal reaction scores (ErD_{50}) of the *B5R*-defective viruses in rabbits. (*B* and *C*) Virulence of the *B5R* defective viruses in SCID mice. RED_{50} and LD_{50} are shown in *B* and *C*, respectively.

weak, as demonstrated by the fact that 10^7 pfu of m8Δ or m8dTM did not elicit any symptoms in SCID mice over a period of 56 days (Fig. 4 *B* and *C*). It should be noted that this dose is 1,000-fold higher than that conferring protective immunity (see Fig. 3*D*). MVA and m8rc were also safe in SCID mice, whereas mO, m8B5R, and Dryvax exhibited lethal pathogenicities at lower doses ($10^{3.5}$, $10^{5.5}$, and $10^{4.5}$ pfu, respectively) (Fig. 4 *B* and *C*).

Discussion

One of our goals is to develop a safe and effective smallpox vaccine and vector virus. The m8 strain could be used as a prototype because it has been proven to induce an effective immune response without serious complications in humans (5, 6). It is important to note that the neurovirulence of these strains was separable from their dermal replicability, as suggested by previous experiments with LO-derived strains expressing the envelope protein of human T cell Leukemia virus type 1 (10).

A major safety drawback of m8 is its spontaneous reversion to the mO-like viruses. We identified the *B5R* gene as being responsible for the reversion, and constructed the *B5R*-defective viruses, m8Δ and m8dTM. These viruses are genetically stable and evidently retain the properties of the highly attenuated m8. Moreover, m8Δ shows a level of immunogenicity similar to that of Dryvax.

A previous study (32) reported that the m8-derived recombinant virus, which expresses the hepatitis B surface antigen, maintained its plaque size during 10 passages in the cell culture. The discrepancy between these data and our results in this study may be due to differences in the cell types used to measure plaque sizes. In the earlier study, plaque assays were performed on PRK cell monolayers on which m8 and mO form plaques that are indistinguishable in size, in contrast to the RK13 cell line used in our study. This may be one reason why the reversion of m8 has been previously undocumented.

Another purpose of this study was to evaluate the importance of *B5R* in generating an immune response that confers protection against smallpox infection. B5R protein and a DNA vaccine expressing *B5R* have been reported to induce production of neutralizing antibodies and achieve partial protection against the virus (22–25). Therefore, we assessed the ability of *B5R*, which is expressed during viral replication in mice, to induce protective immunity. The *B5R* defective virus (m8Δ) was able to elicit neutralizing antibodies, leading to protection comparable to that of the wild-type *B5R*-harboring vaccine, Dryvax. Moreover, the protective efficacies of m8dTM and m8B5R were, unexpectedly, never superior to the *B5R* defective virus (Fig. 3 and Table 2), and m8B5R was statistically inferior to m8Δ. Western blotting confirmed that B5R proteins were expressed by m8dTM, m8B5R, and Dryvax, and that these proteins were immunogenic and could induce anti-B5R antibody production in mice (data not shown). The subtle difference in protection between m8rc and the *B5R* knockout virus may be due to the 10-kDa truncated B5R protein synthesized by m8rc (Fig. 2*B*). These data indicate that B5R does not play a major role in inducing protective immunity in response to live vaccinia inoculation in mice. The clinical trial data on m8 in Japan (5, 6) also support our conclusion.

However, the neutralizing antibody titers induced in mice were correlated with body weight changes to some extent, but not completely. Quantitation of antibody titers by ELISAs against the outer membrane proteins of intracellular matured virion (34, 35), which includes L1R, a major target of neutralizing antibodies, showed a similar tendency with neutralizing antibody titers (data not shown). Moreover, the levels of A33R EEV-specific antibodies in mice, which had been suggested to be important for protective immunity (22, 23), did not correlate with the protection level (data not shown). These results may suggest that there may be a contribution of cell-mediated immunities to the protection (36, 37).

Recently, several groups have reevaluated the available vaccinia strains, including the replication-defective MVA, in a search for safer smallpox vaccines (37–40). Although 10^9 pfu of MVA was shown to be safe in monkeys (41), a large quantity of virus, 10^8 pfu, an amount that is 1,000-fold more than a conventional vaccination dosage, was necessary to induce protective immunity (40). Because m8Δ can replicate in the host, it can induce protective immunity comparable to that of the Dryvax strain at a 100-fold lower dose of the virus, making it clearly more effective than MVA. Moreover, m8Δ was not pathogenic in SCID mice at a dose 1,000-fold greater than the lethal dose of Dryvax, a dose that was also 1,000-fold greater than the dose required for its effective protective immunity. m8Δ replicated at the injection site in rabbit skin, and caused temporary viremia in SCID mice (data not shown). The preliminary experiments suggested that the viral loads of VV correlate with their pathogenicity to SCID mouse. The virus seems to be eliminated rapidly thereafter and seldom replicates in the CNS (5); therefore, the magnitude and the region of replication should be

restricted, which may explain its safety and efficacy. Therefore, m8Δ should be eminently suitable as a safe and effective vaccine virus and viral vector.

We thank Y. Horiuchi (National Institute of Infectious Diseases) for helpful advice on statistical analysis; S. Morikawa for gifts of anti-B5R rabbit sera and viruses; I. K. Damon and J. Becher for Dryvax vaccine; R. Drillien (Institute of Genetics, Molecular and Cell Biology, ●●●) and R. Wittek (University of Lausanne, Lausanne, Switzerland) for recombinant baculoviruses; Y. Nagaoka (National Institute of Infectious Diseases) and K. Eshita (Chiba Serum Institute) for technical advice on animal experiments; and H. Yoshizawa, K. Suzuki, and S. Hashizume for sharing information on the basic characteristics of m8.

AQ: L

AQ: M

AQ: N

1. World Health Organization. (1980) *Wkly. Epidemiol. Rec.* **55**, 148.
2. Henderson, D. A., Inglesby, T. V., Bartlett, J. G., Ascher, M. S., Eitzen, E., Jahrling, P. B., Hauer, J., Layton, M., McDade, J., Osterholm, M. T., *et al.* (1999) *J. Am. Med. Assoc.* **281**, 2127–2137.
3. Reed, K. D., Melski, J. W., Graham, M. B., Regnery, R. L., Sotir, M. J., Wegner, M. V., Kazmierczak, J. J., Stratman, E. J., Li, Y., Fairley, J. A., *et al.* (2004) *N. Engl. J. Med.* **350**, 342–350.
4. Centers for Disease Control and Prevention (CDC). (2004) *Morbid. Mortal. Wkly. Rep.* **53**, 166–167.
5. Hashizume, S., Yoshizawa, H., Morita, M. & Suzuki, K. (1985) in *Vaccinia viruses as Vectors for Vaccine Antigens*, ed. Quinnan, G. V. (Elsevier, Amsterdam), pp. 421–428.
6. Yamaguchi, M., Kimura, M. & Hirayama, M. (1975) *Clin. Virol.* **3**, 269–278.
7. Morita, M., Arita, M., Komatsu, T., Amano, H. & Hashizume, S. (1977) *Microbiol. Immunol.* **21**, 417–418.
8. Morita, M., Aoyama, Y., Arita, M., Amano, H., Yoshizawa, H., Hashizume, S., Komatsu, T. & Tagaya, I. (1977) *Arch. Virol.* **53**, 197–208.
9. Kempe, C. H., Fuliginiti, V., Minamitani, M. & Shinefield, H. (1968) *Pediatrics* **42**, 980–985.
10. Shida, H., Hinuma, Y., Hatanaka, M., Morita, M., Kidokoro, M., Suzuki, K., Maruyama, T., Takahashi-Nishimaki, F., Sugimoto, M., Kitamura, R., *et al.* (1988) *J. Virol.* **62**, 4474–4480.
11. Lee, M. S., Roos, J. M., McGuigan, L. C., Smith, K. A., Cormier, N., Cohen, L. K., Roberts, B. E. & Payne, L. G. (1992) *J. Virol.* **66**, 2617–2630.
12. Kitamura, T., Kitamura, T. & Tagaya, I. (1967) *Nature* **215**, 1187–1188.
13. Takahashi-Nishimaki, F., Funahashi, S., Miki, K., Hashizume, S. & Sugimoto, M. (1991) *Virology* **181**, 158–164.
14. Smith, G. L., Vanderplasschenb, A. & Law, M. (2002) *J. Gen. Virol.* **83**, 2915–2931.
15. Schmelz, M., Sodeik, B., Ericsson, M., Wolffe, E. J., Shida, H., Hiller, G. & Griffiths, G. (1994) *J. Virol.* **68**, 130–147.
16. Hollinshead, M., Rodger, G., Van Eijl, H., Law, M., Hollinshead, R., Vaux, D. J. & Smith, G. L. (2001) *J. Cell Biol.* **154**, 389–402.
17. Rietdorf, J., Ploubidou, A., Reckmann, I., Holmström, A., Frischknecht, F., Zettl, M., Zimmermann, T. & Way, M. (2001) *Nat. Cell Biol.* **3**, 992–1000.
18. Ward, B. M. & Moss, B. (2001) *J. Virol.* **75**, 4802–4813.
19. Katz, E., Ward, B. M., Weisberg, A. S. & Moss, B. (2003) *J. Virol.* **77**, 12266–12275.
20. Newsome, T. P., Scaplehorn, N. & Way, M. (2004) *Science* **306**, 124–129.
21. Payne, L. G. & Kristensson, K. (1985) *J. Gen. Virol.* **66**, 643–646.
22. Galmiche, M. C., Goenaga, J., Wittek, R. & Rindisbacher, L. (1999) *Virology* **254**, 71–80.
23. Hooper, J. W., Custer, D. M. & Thompson, E. (2003) *Virology* **306**, 181–195.
24. Pulford, D. J., Gates, A., Bridge, S. H., Robinson, J. H. & Ulaeto, D. (2004) *Vaccine* **22**, 3358–3366.
25. Hooper, J. W., Thompson, E., Wilhelmsen, C., Zimmerman, M., Ichou, M. A., Steffen, S. E., Schmaljohn, C. S., Schmaljohn, A. L. & Jahrling, P. B. (2004) *J. Virol.* **78**, 4433–4443.
26. Stickl, H., Hochstein-Mintzel, V., Mayr, A., Huber, H. C., Schafer H. & Holzner, A. (1974) *Dtsch. Med. Wochenschr.* **99**, 2386–2392.
27. Mayr, A., Hochstein-Mintzel, V. & Stickl, H. (1974) *Infection* **3**, 6–14.
28. Finney, D. J. (1959) *Acta Microbiol.* **6**, 341–368.
29. Law, M. & Smith, G. L. (2001) *Virology* **280**, 132–142.
30. Herrera, E., Lorenzo, M. M., Blasco, R. & Isaacs, S. N. (1998) *J. Virol.* **72**, 294–302.
31. Jin, N.Y., Funahashi, S. & Shida, H. (1994) *Arch. Virol.* **138**, 315–330.
32. Williamson, J. D., Reith, R. W., Jeffrey, L. J., Arrand, J. R. & Mackett, M. (1990) *J. Gen. Virol.* **71**, 2761–2767.
33. Watanabe, K., Morita, M. & Kojima, A. (1989) *Vaccine* **7**, 499–502.
34. Rodriguez, J. F., Janeczko, R. & Esteban, M. (1985) *J. Virol.* **56**, 482–488.
35. Wolffe, E. J., Vijaya, S. & Moss, B. (1995) *Virology* **211**, 53–63.
36. Xu, R., Johnson, A. J., Liggitt, D. & Bevan, M. J. (2004) *J. Immunol.* **172**, 6265–6271.
37. Wyatt, L. S., Earl, P. L., Eller, L. A. & Moss B. (2004) *Proc. Natl. Acad. Sci. USA* **101**, 4590–4595.
38. Ober, B. T., Bruhl, P., Schmidt, M., Wieser, V., Gritschenberger, W., Coulibaly, S., Savidis-Dacho, H., Gerencer, M. & Falkner, F. G. (2002) *J. Virol.* **76**, 7713–7723.
39. Drexler, I., Staib, C., Kastenmuller, W., Stevanovic, S., Schmidt, B., Lemonnier, F. A., Rammensee, H. G., Busch, D. H., Bernhard, H., Erfle, V., *et al.* (2003) *Proc. Natl. Acad. Sci. USA* **100**, 217–222.
40. Earl, P. L., Americo, J. L., Wyatt, L. S., Eller, L. A., Whitbeck, J. C., Cohen, G. H., Eisenberg, R. J., Hartmann, C. J., Jackson, D. L., Kulesh, D. A., *et al.* (2004) *Nature* **428**, 182–185.
41. Stittelaar, K. J., Kuiken, T., de Swart, R. L., van Amerongen, G., Vos, H. W., Niesters, H. G., van Schalkwijk, P., van der Kwast, T., Wyatt, L. S., Moss, B., *et al.* (2001) *Vaccine* **19**, 3700–3709.

AQ: O

ELSEVIER

Journal of Neuroimmunology 151 (2004) 189–194

Journal of
Neuroimmunology

www.elsevier.com/locate/jneuroim

Short communication

Th1/Th2 balance and HTLV-I proviral load in HAM/TSP patients treated with interferon-α

Juan Feng[a], Tatsuro Misu[a], Kazuo Fujihara[a,*], Naoko Misawa[b], Yoshio Koyanagi[b], Yusei Shiga[a], Atsushi Takeda[a], Shigeru Sato[c], Sadao Takase[c], Takeshi Kohnosu[d], Hiroshi Saito[d], Yasuto Itoyama[a]

[a] *Department of Neurology, Tohoku University School of Medicine 1-1 Seiryomachi, Aobaku, Sendai 980-8574, Japan*
[b] *Department of Microbiology, Tohoku University School of Medicine, Japan*
[c] *Department of Neurology, Kohnan Hospital, Japan*
[d] *Department of Neurology, National Nishitaga Hospital, Japan*

Received 6 October 2003; received in revised form 15 January 2004; accepted 20 February 2004

Abstract

We studied the immunological and virological effects of interferon-α (IFN-α) therapy in nine patients with HTLV-I-associated myelopathy (HAM/TSP). After therapy, the percentages of CCR5+ cells in CD4+ cells significantly decreased in the cerebrospinal fluid as well as blood. The therapy also significantly lowered the intracellular IFN-γ+/interleukin-4+ T-cell ratio in blood. Those helper T-cell type 1 (Th1)-related responses tended to be higher and reduce more evidently following therapy in three patients who clinically improved. Also, all the three patients had one or more HTLV-I copies in five blood mononuclear cells. These results suggest that IFN-α suppresses Th1 responses in HAM/TSP and that the patients with higher Th1 immunity and proviral loads may be responders of the therapy. Larger-scale studies are needed to confirm the findings.

Keywords: HAM/TSP; HTLV-I; Interferon-alpha therapy; Helper T cell; Chemokine receptor

1. Introduction

Human T-lymphotropic virus type I (HTLV-I) is associated with chronic inflammatory myelopathy, HTLV-I-associated myelopathy/tropical spastic paraparesis (HAM/TSP) (Gessain et al., 1985; Osame et al., 1986; Izumo et al., 2000). Previous studies demonstrated remarkable immune activation including helper T-cell type 1 (Th1)-associated responses (Kuroda and Matsui, 1993; Itoyama et al., 1996; Umehara et al., 1994; Jacobson et al., 1998) and high HTLV-I proviral loads (Nagai et al., 1998) in HAM/TSP. These immunological and virological changes are probably important in the pathogenesis of this myelopathy and effective immunotherapies for HAM/TSP need to suppress these abnormalities.

A randomized, double-blind study demonstrated that interferon-α (IFN-α) was clinically effective in HAM/TSP (Izumo et al., 1996). The immunological effects of the therapy had been unclear, but we recently found a significant reduction of CD4 cell subsets in the cerebrospinal fluid (CSF) of the patients receiving the therapy (Feng et al., 2003). Here, we report Th1 and Th2-associated chemokine receptor expression on T cells, intracellular cytokine levels in T cells and HTLV-I proviral loads in blood before and after the therapy in the same patients.

2. Materials and methods

2.1. Subjects

Nine patients (five women and four men) were enrolled in the present study as reported previously (Feng et al., 2003). Their ages ranged from 54 to 72 years old and the duration of disease was from 2 to 50 years. The clinical disability was graded according to the Osame's scale: motor

* Corresponding author. Tel.: +81-22-717-7189; fax: +81-22-717-7192.
E-mail address: fujikazu@em.neurol.med.tohoku.ac.jp (K. Fujihara).

0165-5728/$ - see front matter © 2004 Elsevier B.V. All rights reserved.
doi:10.1016/j.jneuroim.2004.02.007

disability: grade 0 (normal)–13 (bedridden), dysuria: grade 0 (normal)–3 (severe) (Izumo et al., 1996). The patients received intramuscular injections of IFN-α (3 million units) daily for 4 weeks (Izumo et al., 1996). None had received immunosuppressants for the last 3 months except for a single patient (HAM3) who was treated with a fixed dose of oral prednisolone (20 mg/day) throughout the therapy. Age- and sex-matched nine HTLV-I-seronegative control subjects were studied for peripheral blood mononuclear cells (PBMC). We obtained informed consents prior to the study and the present study conformed to the guidelines of Medical Ethics Committee of our medical school.

2.2. Mononuclear cell preparation

Heparinized venous blood and CSF were collected before the IFN-α therapy and the next day of the last IFN-α injection. PBMC were isolated by Ficoll-Paque and CSF cells were directly isolated by centrifugation.

2.3. Flow cytometric analysis

2.3.1. T-cell subset

We analyzed T-cell subsets using a standard direct immunofluorescent technique with monoclonal antibodies (MoAbs), a three-color flow cytometer (FACSCalibur, Becton Dickinson, San Jose, CA) and the CellQuest software.

The analyzed subsets were CCR5+ and CXCR3+ (helper T-cell type 1 [Th1]-associated chemokine receptor expressing cells) and CCR3+ (Th2-associated chemokine receptor expressing cells, especially in the early stage of Th2 response) among CD4+ and CD8+ cells. Peridinin chlorophyll protein-conjugated anti-CD4 and anti-CD8, fluorescein isothiocyanate-conjugated anti-CD8 MoAbs were provided by Becton Dickinson. Phycoerythrin-conjugated anti-CCR5 and anti-CCR3 and carboxy-fluorescein succinimidylester-conjugated anti-CXCR3 MoAbs were purchased from Dako (Tokyo, Japan).

The data were expressed as the percentages of T-cell subsets in CD4+ or CD8+ cells.

2.3.2. Intracellular Th1/Th2-associated cytokines

The ratio of IFN-γ producing cells to interleukin-4 (IL-4) producing cells in CD3+ cells was assayed with a FACSCalibur according to the previous report (Pala et al., 2000).

2.4. HTLV-I proviral load in PBMC

DNA was extracted from PBMC. The HTLV-I proviral load was quantified using a real-time Taq-Man PCR method (PE Applied Biosystems, Foster City, CA). Standard curves of β-actin and HTLV-I tax genes were generated using DNA derived from an HTLV-I infected cell line, TloM1. TaqMan amplifications were carried out with the forward primers 5′-ACTCCTCAAGCGAGCTGCAT-3′, the reverse primer 5′-TTTTTCTTTGGGATCGGCG-3′ (Greiner Japan, Tokyo, Japan) and HTLV-I TaqMan Probe 5′-CCCAAGACCC-GTCGGAGGCC-3′ labeled with the 5′ FAM reporter dye and the 3′ TAMRA quencher dye molecules (Japan BioService, Asaka, Japan). The primers and probe for β-actin gene were obtained from PE Applied Biosystems. The thermal cycle conditions were 50 °C for 2 min followed by 95 °C for 10 min (hot start) and then 40 cycles were run by melting at 95 °C for 15 s and annealing/extension at 60 °C for 1 min in each cycle. Each sample was analyzed in triplicate. For each reaction, 100 ng of DNA, the equivalent of 2×10^4 cells, were subjected to the analysis. The amplifications were performed on an ABI PRISM 7700 sequence detector equipped with a 96-well thermal cycler. Copy numbers were reported as copy equivalents per 10^5 PBMC.

2.5. Statistical analysis

We used Mann–Whitney *U*-test to compare the unpaired values, Wilcoxon's signed rank test to compare the paired values. We also examined correlations in clinical disability, immunological and virological parameters (motor disability grade, percentages of CCR5+, CXCR3+ and CCR3+ in CD4+ cells, and CCR5+, CXCR3+ and CCR3+ in CD8+ cells in the CSF and blood, ratio of IFN-γ producing cells to IL-4 producing cells in blood CD3+ cells, and HTLV-I proviral load) of the HAM/TSP patients with Spearman rank correlation coefficient test. Correlations in both baseline values and the changes after the IFN-α therapy were analyzed. *P*-values less than 0.05 were considered statistically significant.

3. Results

3.1. Clinical effects

The motor disability grade improved in three patients after the IFN-α therapy (Patients HAM 3, grade 3 → 2; HAM 5, grade 8 → 6; HAM 6, grade 6 → 4) as we reported (Feng et al., 2003). The dysuria grade did not change.

3.2. T-cell subsets (Table 1)

3.2.1. CCR5

The percentage of CCR5+ cells in blood CD4+ cells was significantly higher before the IFN-α therapy in HAM/TSP than in control. In HAM/TSP, the mean percentages of all CCR5+ T-cell subsets in blood and CSF decreased after the therapy. Among them, the percentage of CCR5+ cells in blood CD4+ cells of HAM/TSP significantly decreased after the therapy, and they were no longer different between HSM/TSP and control. The percentage of CCR5+ cells in CSF CD4+ cells also significantly decreased after the therapy (Table 1).

Table 1
T cells expressing Th1/Th2-associated chemokine receptors in HAM/TSP patients treated with interferon-α and in control subjects

	CCR5+ in CD4+	CXCR3+ in CD4+	CCR3+ in CD4+
Control (n=9)	(%)	(%)	(%)
Blood	0.5 ± 0.1	27.3 ± 4.8	0.3 ± 0.1
HAM/TSP (n=9)			
Blood			
before IFN-α	1.5 ± 0.9 *	27.9 ± 12.3	0.3 ± 0.2
after IFN-α	0.9 ± 0.8 *	25.5 ± 7.6	0.4 ± 0.2
CSF			
before IFN-α	20.5 ± 8.8 *	88.5 ± 5.4	4.3 ± 4.3
after IFN-α	13.4 ± 5.3 *	81.3 ± 12.2	7.5 ± 3.1
	CCR5+ in CD8+	CXCR3+ in CD8+	CCR3+ in CD8+
Control (n=9)	(%)	(%)	(%)
Blood	0.9 ± 0.9	35.9 ± 8.1 *	0.5 ± 0.2
HAM/TSP (n=9)			
Blood			
before IFN-α	3.0 ± 4.5	55.5 ± 17.4 *	0.7 ± 0.4
after IFN-α	1.6 ± 1.0	36.4 ± 17.6 *	0.6 ± 0.2
CSF			
before IFN-α	27.1 ± 12.1	94.8 ± 4.4	4.3 ± 4.3
after IFN-α	17.9 ± 6.5	90.3 ± 9.3	7.5 ± 3.6

Data are mean percentages ± standard deviation.
*$P < 0.05$.

The percentage of CCR5+ cells in CSF CD4 cells was unequivocally higher in the three patients who clinically improved after the therapy (the lowest value was 26.8% in Patient HAM 6) than in the six patients without clinical effect (the highest value was 18.3% in Patient HAM 2).

3.2.2. CXCR3

In blood, the percentages of CXCR3+ cells in CD8+ cells were significantly higher in HAM/TSP before the therapy than in control. In HAM/TSP, the mean percentages of all CXCR3+ T-cell subsets in blood and CSF decreased after the therapy. Among them, the percentage of CXCR3+ cells in CD8+ cells significantly decreased after the therapy in HAM/TSP, and it was no longer different between HAM/TSP and control.

3.2.3. CCR3

No CCR3+ subset was significantly different between HAM/TSP and control or changed significantly after the therapy in HAM/TSP, although the mean percentages of CCR3+ cells in CSF CD4+ and CD8+ cells increased after the therapy.

3.3. Intracellular TH1/TH2-associated cytokines (Fig. 1)

The IFN-α therapy significantly decreased the ratio of intracellular IFN-γ- versus IL-4-producing T cells in blood (9.5 ± 7.6 before the therapy and 5.8 ± 4.9 after the therapy). The ratios in the three patients who clinically improved following the therapy (Patients HAM 3, 5 and 6) were over 5.0, while the therapy was not effective in any of the four patients with the ratios being less than 5.0 (Patients HAM 9, 4, 1 and 7).

3.4. HTLV-I proviral load (Fig. 2)

The HTLV-I proviral copy number before the IFN-α therapy in the nine patients was 13272 ± 9006 copies and

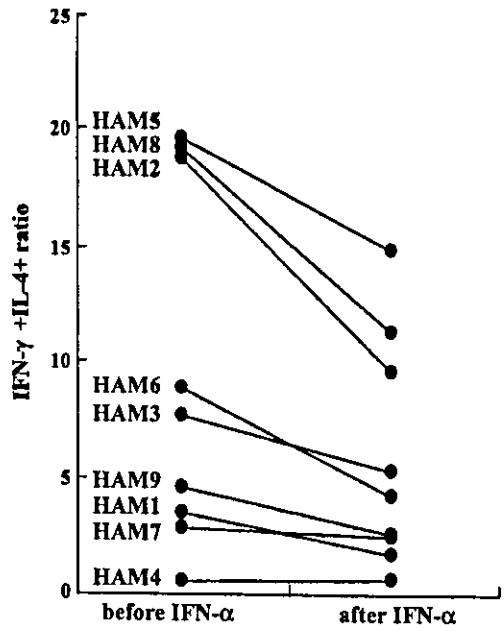

Fig. 1. Intracellular Th1/Th2 cytokine balance in T cells of the patients with HAM/TSP treated with IFN-α. The ratio of IFN-γ+ cells to IL-4+ cells among CD3+ T cells was significantly lower after the IFN-α therapy. Before-IFN-α, before IFN-α therapy; after-IFN-α, after IFN-α therapy.

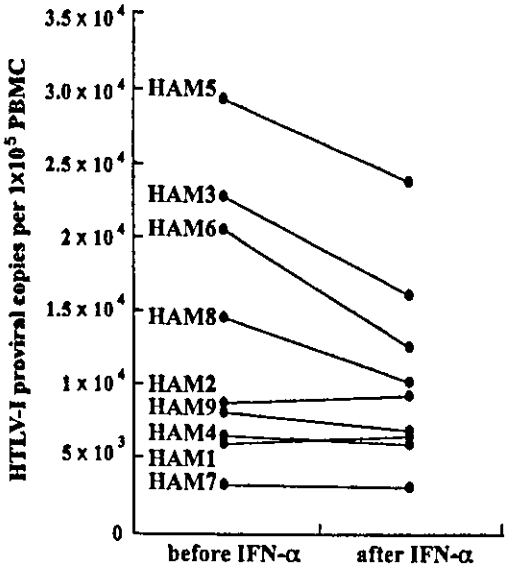

Fig. 2. HTLV-I proviral loads in the PBMC of the patients with HAM/TSP treated with IFN-α. After the IFN-α therapy, HTLV-I proviral loads apparently decreased in the patients with higher proviral loads, and clinical effect was seen in the three patients with 2×10^4 copies or more in 10^5 PBMC (HAM3, HAM5 and HAM6). Before-IFN-α, before IFN-α therapy; after-IFN-α, after IFN-α therapy.

that after the therapy was 10472 ± 6323 copies ($P = 0.06$). Patients HAM 3, 5, 8 and 6, who had the highest proviral loads and who experienced the most obvious decline in proviral load as a result of therapy, were among the ones with the highest baseline ratios of intracellular IFN-γ- versus IL-4-producing blood T cells and with the most dramatic decline in those values following the therapy (Fig. 1). Furthermore, three of these four patients were the ones who clinically improved, and all the three patients had 2×10^4 HTLV-I copies or more in 10^5 PBMC. Meanwhile, clinical effect was not seen in any patient with lower HTLV-I proviral load and their proviral loads remained unchanged after the therapy (Fig. 2).

3.5. Correlation

None of the correlations in clinical disability, immunological and virological parameters in the HAM/TSP patients was statistically significant.

3.6. Comparison of immunological and virological findings in responders and non-responders to IFN-α therapy

We compared the immunological and virological findings in responders (Patients HAM 3, 5 and 6) and non-responders (Patients HAM 1, 2, 4, 7, 8 and 9) to the IFN-α therapy (Table 2). We could not analyze the data statistically due to the small sample size. However, among the significant parameters in the statistical analyses of HAM/TSP patients, there was a tendency for the percentages of CCR5+ cells in CD4+ cells in the CSF and blood, the ratio of intracellular IFN-γ- versus IL-4-producing T cells in blood, and the HTLV-I proviral load to be higher and reduce more evidently following the therapy in responders as compared with non-responders. In the other parameters, the percen-

Table 2
Immunological and virological data in "responders" and "non-responders" to the interferon-α therapy

	CCR5+ in CD4+ (%)	CXCR3+ in CD4+ (%)	CCR3+ in CD4+ (%)	CCR5+ in CD8+ (%)	CXCR3+ in CD8+ (%)	CCR3+ in CD8+ (%)	IFN-γ/ IL-4 ratio	HTLV-I proviral load (copies/10^5 PBMC)
Blood								
Responders								
(A) Before therapy	2.0 ± 1.1	28.7 ± 7.8	0.4 ± 0.1	5.6 ± 7.6	49.1 ± 21.2	0.5 ± 0.1	11.8 ± 6.1	24156 ± 4666
(B) After therapy	1.1 ± 0.3	23.3 ± 4.8	0.4 ± 0.2	2.1 ± 1.0	37.2 ± 17.4	0.6 ± 0.4	6.4 ± 2.9	17506 ± 5694
(A)–(B)	0.9 ± 0.4	6.4 ± 7.6	0.0 ± 0.1	3.5 ± 6.6	11.8 ± 4.0	0.1 ± 0.2	5.4 ± 3.5	6650 ± 1107
Non-responders								
(A) Before therapy	1.2 ± 0.8	26.1 ± 10.9	0.4 ± 0.1	1.7 ± 1.7	51.2 ± 19.0	0.8 ± 0.5	8.3 ± 8.7	7830 ± 3802
(B) After therapy	1.0 ± 1.0	26.0 ± 8.8	0.4 ± 0.1	1.3 ± 1.0	37.4 ± 17.6	0.5 ± 0.1	5.6 ± 5.9	6954 ± 2538
(A)–(B)	0.4 ± 0.2	2.4 ± 3.2	0.1 ± 0.2	0.5 ± 0.0	13.8 ± 10.1	0.2 ± 0.5	2.7 ± 3.0	876 ± 1851
CSF								
Responders								
(A) Before therapy	33.5 ± 9.0	92.7 ± 0.8	8.8 ± 5.7	35.4 ± 17.1	97.8 ± 3.1	6.1 ± 2.8		
(B) After therapy	19.4 ± 3.0	89.5 ± 3.2	9.0 ± 4.6	25.4 ± 19.7	96.8 ± 0.5	7.5 ± 1.4		
(A)–(B)	14.1 ± 5.9	3.1 ± 4.0	−0.2 ± 1.1	9.9 ± 19.0	1.0 ± 2.6	−1.5 ± 1.3		
Non-responders								
(A) Before therapy	15.3 ± 2.0	86.8 ± 5.6	2.1 ± 0.6	23.9 ± 9.9	93.6 ± 4.5	3.1 ± 2.9		
(B) After therapy	10.9 ± 4.0	78.0 ± 13.2	6.1 ± 0.2	15.9 ± 5.3	87.9 ± 9.0	7.6 ± 5.0		
(A)–(B)	4.2 ± 2.4	8.8 ± 17.4	−4.5 ± 0.4	8.9 ± 12.2	5.8 ± 11.2	−4.8 ± 6.2		

Data are shown as mean ± standard deviation.
IFN-γ, interferon-gamma; IL-4, interleukin-4; IFN-γ/IL-4, ratio of IFN-γ producing cells to IL-4 producing cells in CD3+ cells; PBMC, peripheral blood mononuclear cells; CSF, cerebrospinal fluid.

tages of CCR3+ cells in CSF CD4+ and CD8+ cells tended to be lower and increase more after the therapy in non-responders than in responders.

4. Discussion

Our previous analysis revealed a significant reduction of CD4+ cells in CSF of HAM/TSP after IFN-α therapy (Feng et al., 2003). In the present study, we focused on the Th1/Th2 balance and showed that IFN-α therapy significantly reduced CCR5+CD4+ cells, a Th1 subset, in the patients' CSF as well as blood. The CCR5+CD4+ cell subset in CSF reflects the disease activity in multiple sclerosis (Misu et al., 2001). This subset is increased in the synovium of active rheumatoid arthritis (Mack et al., 1999), and the inhibition of CCR5 successfully treated adjuvant arthritis in rats, an animal model of rheumatoid arthritis (Barnes et al., 1998). In HAM/TSP, elevated levels of CCR5 on memory CD4+ cells in PBMC (Wu et al., 2000) and macrophage inflammatory protein-1α, a CCR5 ligand, in CSF (Miyagishi et al., 1995) were reported. These findings suggest a pathogenic role of CCR5+CD4+ cells in HAM/TSP and other immunologic diseases, and a suppression of the subset by IFN-α might relate to the alleviation of myelitis in HAM/TSP.

There was also a tendency for the CXCR3+CD4 cell, another Th1 subset, to be decreased and CCR3+CD4+ cells, a Th2 subset, to be increased in CSF of the treated patients. A significant decrease in blood CD8+ cell number in the treated patients (Feng et al., 2003) may be attributable to the reduction in CXCR3+CD8+ cells. Moreover, intracellular Th1/Th2-associated cytokine ratio in T cells, which was analyzed only in blood because of the limited volumes of CSF, reduced significantly following the therapy. Taken together, our data suggests that the IFN-α therapy suppressed Th1-related responses in HAM/TSP, although our small-scale study did not address whether the immunological changes were directly associated with the clinical efficacy of IFN-α in HAMTSP.

The present study suggested some interesting differences in baseline immunological and virological findings between responders and non-responders to the IFN-α therapy, that is, responders showed higher Th1 responses and more viral replication than non-responders, and the therapeutic suppression to those parameters was more evident in responders. Our small-scale study could not confirm the associations statistically, but those analyses will be critically important to reliably predict therapeutic efficacy of intramuscular injections of IFN-α beforehand. Whether such laboratory data as (1) baseline percentage of CCR5+ cells in CSF CD4+ cells >20%, (2) baseline ratio of intracellular IFN-γ- versus IL-4-producing blood T cells >5.0 and (3) baseline HTLV-I proviral load more than one copy in five PBMC are really linked to clinical efficacy of IFN-α therapy in HAM/TSP need to be examined in a larger cohort of patients by statistical analyses.

Acknowledgements

The authors thank Mr. Brent Bell for reading the manuscript. This work was supported by the grants from the Ministry of Education, Science, Culture, Sports and Technology and the Tawara's Endowment for HAM Research.

References

Barnes, D.A., Tse, J., Kaufhold, M., Owen, M., Hesselgesser, J., Strieter, R., Horuk, R., Perez, H.D., 1998. Polyclonal antibody directed against human RANTES ameliorates disease in the Lewis rat adjuvant-induced arthritis model. J. Clin. Invest. 101, 2910–2919.

Feng, J., Misu, T., Fujihara, K., Saito, H., Takahashi, T., Kohnosu, T., Shiga, Y., Takeda, A., Sato, S., Takase, S., Itoyama, Y., 2003. Interferon-alpha significantly reduces cerebrospinal fluid CD4 cell subsets in HAM/TSP. J. Neuroimmunol. 141, 170–173.

Gessain, A., Barin, F., Vernant, J.C., Gout, O., Maurs, L., Calender, A., de The, G., 1985. Antibodies to human T-lymphotropic virus type-I in patients with tropical spastic paraparesis. Lancet 2, 407–410.

Itoyama, Y., Kira, J., Fujii, N., Goto, I., Yamamoto, N., 1996. Increases in helper inducer T cells and activated T cells in HTLV-I-associated myelopathy. Ann. Neurol. 26, 257–262.

Izumo, S., Goto, I., Itoyama, Y., Okajima, T., Watanabe, S., Kuroda, Y., Araki, S., Mori, M., Nagataki, S., Matsukura, S., Akamine, T., Nakagawa, M., Yamamoto, I., Osame, M., 1996. Interferon-alpha is effective in HTLV-I-associated myelopathy: a multicenter, randomized, double-blind, control trial. Neurology 46, 1016–1021.

Izumo, S., Umehara, F., Osame, M., 2000. HTLV-I-associated myelopathy. Neuropathology 20, S65–68 (Suppl).

Jacobson, S., Levin, M., Utz, U., Drew, P., 1998. Infectious immune disorders: HTLV-I. In: Antel, J.P., Birnbaum, G., Hartung, H.P. (Eds.), Clinical neuroimmunology. Blackwell, Malden, pp. 204–217.

Kuroda, Y., Matsui, M., 1993. Cerebrospinal fluid interferon-gamma is increased in HTLV-I-associated myelopathy. J. Neuroimmunol. 42, 223–236.

Mack, M., Bruhl, H., Gruber, R., Jaeger, C., Cihak, J., Eiter, V., Plachy, J., Stangassinger, M., Uhlig, K., Schattenkirchner, M., Schlondorff, D., 1999. Predominance of mononuclear cells expressing the chemokine receptor CCR5 in synovial effusions of patients with different forms of arthritis. Arthritis Rheum. 42, 981–988.

Misu, T., Onodera, H., Fujihara, K., Matsushima, K., Yoshie, O., Okita, N., Takase, S., Itoyama, Y., 2001. Chemokine receptor expression on T cells in blood and cerebrospinal fluid at relapse and remission of multiple sclerosis: imbalance of Th1/Th2-associated chemokine signaling. J. Neuroimmunol. 114, 207–212.

Miyagishi, R., Kikuchi, S., Fukazawa, T., Tashiro, K., 1995. Macrophage inflammatory protein-1 alpha in the cerebrospinal fluid of patients with multiple sclerosis and other inflammatory neurological diseases. J. Neurol. Sci. 129, 223–227.

Nagai, M., Usuku, K., Matsumoto, W., Kodama, D., Takenouchi, N., Moritoyo, T., Hashiguchi, S., Ichinose, M., Bangham, C.R., Izumo, S., Osame, M., 1998. Analysis of HTLV-I proviral load in 202 HAM/TSP patients and 243 asymptomatic HTLV-I carriers: high proviral load strongly predisposes to HAM/TSP. J. Neurovirol. 4, 586–593.

Osame, M., Usuku, K., Izumo, S., Ijichi, N., Amitani, H., Igata, A., Matsumoto, M., Tara, M., 1986. HTLV-I associated myelopathy, a new clinical entity. Lancet 1, 1031–1032.

Pala, P., Hussell, T., Openshaw, P.J., 2000. Flow cytometric measurement of intracellular cytokines. J. Immunol. Methods 243, 107–124.

Umehara, F., Izumo, S., Ronquillo, A.T., Matsumuro, K., Sato, E.,

Osame, M., 1994. Cytokine expression in the spinal cord lesions in HTLV-I-associated myelopathy. J. Neuropathol. Exp. Neurol. 53, 72–77.

Wu, X.M., Osoegawa, M., Yamasaki, K., Kawano, Y., Ochi, H., Horiuchi, I., Minohara, M., Ohyagi, Y., Yamada, T., Kira, J.I., 2000. Flow cytometric differentiation of Asian and Western types of multiple sclerosis, HTLV-I-associated myelopathy/tropical spastic paraparesis (HAM/TSP) and hyperIgEaemic myelitis by analyses of memory CD4 positive T cell subsets and NK subsets. J. Neurol. Sci. 177, 24–31.

Available online at www.sciencedirect.com
SCIENCE DIRECT
Microbes and Infection 6 (2004) 715–724
Microbes and Infection
www.elsevier.com/locate/micinf

Original article

Role of Nup98 in nuclear entry of human immunodeficiency virus type 1 cDNA

Hirotaka Ebina [a], Jun Aoki [a], Shunsuke Hatta [a], Takeshi Yoshida [a], Yoshio Koyanagi [b,*]

[a] Department of Virology, Tohoku University Graduate School of Medicine, Sendai 980-8575, Japan
[b] Laboratory of Viral Pathogenesis, Institute for Virus Research, Kyoto University, 53 Shougoin-kawahara machi, Sakyou-ku, Kyoto 606-8507, Japan

Received 18 February 2004; accepted 7 April 2004

Available online 24 May 2004

Abstract

Human immunodeficiency virus type 1 (HIV-1), like other lentiviruses, can infect non-dividing cells. The lentiviruses are most likely to have evolved a nuclear import strategy to import HIV-1 cDNA and viral protein complex through the nuclear pore complex (NPC) formed by nucleoporin proteins (Nup). In this study, we found that synthesis of integrated and 2LTR but not full-length form of HIV-1 cDNA was clearly impaired in culture via transduction of vesicular stomatitis virus matrix protein (VSV M), an inhibitor protein, through binding to the phenylalanine-glycine (FG) repeat region of Nup98. The impairment of synthesis of integrated and 2LTR DNA with VSV M was restored by ectopic overexpression of Nup98. A series of experiments using Nup98-depleted NPC by the small interfering RNA (siRNA) technique showed specific impairment of NPC structure and some functions, including nuclear import of HIV-1 cDNA. Our results suggest that Nup98 on the NPC specifically participates in the nuclear entry of HIV-1 cDNA following HIV-1 entry.

Keywords: Nucleoporin; NPC; HIV-1; Nuclear import

1. Introduction

The Retroviridae family of viruses can reverse transcribe their RNA genome into cDNA and then integrate the cDNA into host chromosomes. The lentiviruses (e.g. HIV) are distinguished by their ability to infect non-dividing cells, whereas the gamma-retroviruses (e.g. Moloney murine leukemia virus) require nuclear membrane dissolution to access the host cell DNA [1]. Thus, the lentiviruses are most likely to have evolved a nuclear import strategy, which allows their cDNA to cross the nuclear membrane independently of mitosis. In the case of human immunodeficiency virus type 1 (HIV-1), mitosis-independent replication was initially shown in terminally differentiated macrophages in vitro [1–3]. The mitosis-independent replication of HIV has also enabled the generation of integration-competent gene transfer vectors with promising therapeutic applications in a variety of non-dividing cellular hosts, including neurons [4], myocytes [5], and retinal cells [6]. To facilitate integration into a host DNA, a preintegration complex (PIC) is generated in the cytoplasm immediately after completion of reverse transcription. The PIC can be isolated successfully from in vitro freshly HIV-1-infected or HIV vector-infected cells and was recently shown to have the ability to traverse the nuclear pore complex (NPC) [1,7]. The NPCs serve as the conduits for bi-directional transport of macromolecules. Translocation across the NPC into the nucleus and from the nucleus into the cytoplasm is governed by a class of proteins known as importins and exportins (transport receptors), respectively. Both are members of the karyopherin family. The transport receptors engage the appropriate import or export signals and mediate their transport [8,9]. The PIC contains a double-strand linear cDNA as well as at least four viral proteins: matrix (MA), reverse transcriptase (RT), integrase (IN), and viral protein R (VPR), and has a diameter of approximately 56 nm, which greatly exceeds the 25 nm central channel of the NPC [1,7,10]. The NPC has a large supramolecular structure formed of ~50 unique proteins in eukaryotic cells, termed nucleoporins (Nup) [8,9,11,12]. High-resolution electron microscopic images of NPCs reveal an eightfold

* Corresponding author. Tel.: +81-75-751-4811; fax: +81-75-751-4812.
E-mail address: ykoyanag@virus.kyoto-u.ac.jp (Y. Koyanagi).

doi:10.1016/j.micinf.2004.04.002

symmetric structure, formed by nuclear and cytoplasmic rings and central spoke complex. The Nups often contain multiple phenylalanine-glycine (FG) dipeptide repeats clustered in domains, which in vertebrates are glycosylated by addition of *O*-linked *N*-acetylglucosamine (GlcNAc). Some of these Nups are localized asymmetrically at the NPC [9,11]. The asymmetric distribution of nucleoporins and the different affinities for import and export complexes may be important in determining the direction of transport [13,14]. Recent studies reported that importin 7 is involved in the nuclear entry of HIV-1 PIC as one of the main transport receptors [15]. However, the steps involved in the NPC remain largely undefined. In the present study, we show that nuclear import of HIV-1 cDNA requires NPC, and Nup98 has a role in nuclear entry of HIV-1 cDNA.

2. Materials and methods

2.1. Chemical treatment

Aphidicolin (APH) (Sigma Chemical Co., St. Louis, MO, USA), actinomycin D (ActD) (Sigma), zidovudine (AZT) (Sigma) or leptomycine B (LMB) (Sigma) was used. APH treatment (5 μg/ml) started 24 h before HIV-1 vector infection. AZT treatment started at the time of infection. LMB was added 2 h after infection. ActD was added 5 h after infection. DNA was extracted 24 h after infection.

2.2 Transfection

Human 293T cells were maintained in D-MEM containing 10% fetal calf serum (FCS). 293T cells were transfected with vesicular stomatitis virus matrix protein (VSV M)-, Nup98- or small interfering RNA (siRNA)-expressing DNA using calcium phosphate methods.

2.3. Quantitative polymerase chain reaction (PCR) assay

For the detection and quantification of individual forms of HIV-1 DNA, full-length/1LTR circle, 2LTR circle and integrated forms, we used a set of primer pairs and fluorogenic probes, as described previously [16,17]. PCR was performed using an ABI PRISM 7700 sequence detection system (PE-Applied Biosystems, Foster City, CA, USA) and TaqMan Universal PCR Master Mix (PE-Applied Biosystems). Cycling conditions included a hot start (50 °C for 2 min, 95 °C for 10 min), followed by 40 cycles of denaturation (95 °C for 15 s) and extension (60 °C for 1 min). To measure the integrated DNA, an *Alu*-sequence-specific sense primer and an antisense HIV-specific primer were used in the first PCR and subsequently 1000-fold diluted products were subjected to real-time PCR assay for measurement of R/U5 DNA, as described previously [16,17].

2.4. Cell-cycle analysis

Cell-cycle progression was examined by single-color flow cytometric analysis of the DNA content stained with 50 μg/ml of propidium iodine (Sigma).

2.5. DNA constructs and recombinant protein expression

Small interference RNA (siRNA)-expressing plasmid DNAs were constructed using the method described by Miyagishi and Taira [18]. The sequences inserted in the *Bfu*AI site of pU6i cassette, immediately downstream of the U6 promoter, were as follows: Nup98-targeted siRNA (siN98), 5′-CACCGAATATGAAAG*T*AAGT*T*A*T*TATAGAATTACATCAAGGGAGATTAGTGACTTGCTTTCATATTCTTTTTTATGC-3′; firefly luciferase-targeted siRNA (siLuc), 5′-CACCGTGCG*T*TG*T*TGGTG*T*TAA*T*CCATCTCCCTTGATGTAATTCTAGGGTTGGCACCAGCAGCGCACTTTTTATGC-3′. Bold-lettered nucleotides are the siRNA sequences, italic nucleotides are mutated, and underlined nucleotides are loop sequences. The siRNA-expressing DNA fragment was also inserted into the *Eco*RI site of a lentivirus vector DNA, pCS-CDF-EH2K^k, and an enhanced green fluorescence protein (EGFP) fragment between the *Age*I and *Xho*I sites of pCS-CDF-EG-PRE [19] was replaced with a H-2K^k fragment (Daiichi pure chemicals, Tokyo, Japan).

HA-tagged human Nup98-expressing plasmid DNA (p37R-HANup98) and EGFP-fused VSV M-expressing DNA (pEGFPN3-M) [20] were kindly provided by Dr. Elisa Izaurralde (European Molecular Biology Laboratory). A *Bss*HII-*Xho*I DNA fragment covering the coding region of HA-tagged human Nup98 region was cloned into a site downstream of CMV promoter in pcDNA3.1/Zeo (+) (Invitrogen, Carlsbad, CA, USA) (pcDNup98). Alanine substitutions from Asp-Thr-Tyr at the position of VSV M 52–54 [VSV (M)] were introduced using an oligonucleotide-directed in vitro mutagenesis system (Quickchange site-directed mutagenesis, Stratagene, San Diego, CA, USA). DsRed-fusion recombinant protein with NLS, U1A and rpL23a was produced in *Escherichia coli*. A double-strand synthetic nucleotide of SV40 NLS (5′-CCA TGC ATA TGC CAA AAA AGA AGA GAA AGG TTG-3′) and PCR-amplified DNA fragment of U1A (1–486), or rpL23a (1–486) from mRNA of HeLa cells was cloned into the *Sma*I or *Sal*I-*Bam*HI sites of pDsRed1-N1 (Clontech, Palo Alto, CA, USA), and then a *Sal*I-*Not*I fragment was inserted in the *Sal*I-*Not*I site of pGEX-4T-2 (Amersham Pharmacia Biotech, Piscataway, NJ, USA). *E. coli* ER2566 (New England Biolabs Inc., Beverly, MA, USA) was used, and recombinant proteins were purified on glutathione sepharose 4 Fast Flow (Amersham) by standard protocols, as previously described [21].

2.6. Reverse-transcription PCR

Total RNA was extracted from transiently transfected cells by using a RNeasy RNA-preparation Kit (Qiagen, KJ

Venlo, The Netherlands). Reverse transcription and PCR were carried out using a SuperScript One-Step RT-PCR with Platinum Taq (Invitrogen). We used the following primers to detect the specific transcripts: for Nup107, 5′-AAACGCG-GTAGCTAAACTGCA-3′, 5′-ACCACCAGCTGACTT-TGTCGA-3′; for Nup214, 5′-CTTGCCACGAAAAC-CGTGA-3′, 5′-CAACCCGCAGTCCTGAAAA-3′; for p62, 5′-CAGACACCGACGGATTTGCTT-3′, 5′-TGGATGTTG-TTGTGGAGGTGC-3′; for Nup98, 5′-TCTCATCCCAA-AACAATGCCTT-3′, 5′-AAACAAAGATGCCTGTCC-AGCA-3′; for Nup153, 5′-TGACAATGAAGAGCC-AAAGTGT-3′, 5′-TAGGAGTTGTTCCAGAGCCAAA-3′. TaqMan GAPDH Control Reagents (PE-Applied Biosystems) were used as primer sets for glyceraldehyde 3-phosphate dehydrogenase (GAPDH). Fifty nanograms of template RNA and 10 pmol of specific primers were used. The efficiency of PCR amplification was roughly in the linear range, as determined by preliminary test with increasing number of cycles. Finally, the PCR products were analyzed by agarose gel electrophoresis using standard techniques.

2.7. Virus vector infection

For HIV-1 vector preparation, a replication-incompetent EGFP-expressing lentivirus (pCS-CDF-CG-PRE) or siRNA-expressing lentivirus was co-transfected into 293T cells along with VSV G-expressing plasmid (pVSV G), HIV-Gag-Pol-expressing plasmid (pRRE) and Rev-expressing plasmid (pRSV-Rev) as described before [6,19]. Three days after transfection, the culture supernatants were cleared by filtration and concentrated through centrifugation at 6000 × *g* for 16 h at 4 °C. The transducing unit (TU) was determined by measurement of EGFP-, or H-2K^k-expressing cells using flow cytometry. Phycoerythrin-labeled anti-mouse H-2K^k monoclonal antibody (mAb) (Cedarlane, Ontario, Canada) was used. Cells were analyzed on FACS SCAN, using Cell Quest software (BD PharMingen, San Diego, CA, USA). Treatment with DNaseI (20 μg/ml) was performed to remove plasmid DNA in the virus stocks. Heat-inactivated (65 °C, 30 min) virus liquid was used as negative control for HIV DNA quantification in infected cells. APH-treated MT-2 cells or 293T cells (2×10^5 cells) were infected with HIV-1 vector (4×10^5 TU). Two hundred thousand 293T cells were transfected with VSV M- or Nup98-expressing DNA and then 24 h later, infected with HIV-1 vector (4×10^5 TU). Two hundred thousand 293T cells were transfected with siRNA-expressing DNA and then 72 h later, infected with HIV-1 vector (4×10^5 TU). The amount of viral DNA was measured by the quantitative PCR assay 24 h after infection, as described above. HeLa cells (1×10^5 cells), grown on cover-slips, were infected with siRNA-expressing HIV-1 vector at multiplicity of infection (m.o.i.) of 1. The cells were analyzed 96 h later by immunofluorescence, immunoblotting or nuclear import assay.

2.8. Immunofluorescence analysis

HeLa cells, grown on cover-slips, were washed twice with phosphate-buffered solution (PBS) and fixed in 4% (vol/vol) paraformaldehyde/PBS for 15 min at room temperature. The cells were permeabilized with 0.2% Triton X-100/PBS for 5 min. After blocking with 5% bovine serum albumin (BSA)/0.1% Triton X/PBS for 1 h, the cells were incubated with an NPC-specific mouse mAb, mAb414 (BabCO, Berkeley, CA, USA) or anti-Nup98 polyclonal antibody (C-16) (Santa Cruz Biotechnology Inc., Santa Cruz, CA, USA) at 4 °C overnight. Cells were washed three times with 0.05% Triton X/PBS and then incubated with Alexa 594-conjugated goat anti-mouse IgG antibody (Molecular Probes, Eugene, OR, USA) or fluorescein isothiocyanate (FITC)-conjugated donkey anti-goat IgG antibodies (Chemicon, Temecula, CA, USA) for 1 h. Cells were washed three times with 0.05% Triton X/PBS, mounted in Vectashield mounting medium for fluorescence (Vector Laboratories, Burlingame, CA, USA) and analyzed with a Leica QFluoro system. The cells were also stained with Hoechst 33342 (Molecular Probes).

2.9. Nuclear import assay

HeLa cells grown on cover-slips were washed in PBS and permeabilized for 5 min on ice in 50 μg/ml digitonin (Sigma)/transport buffer (20 mM Hepes–NaOH, pH 7.3, 110 mM CH_3COOK, 2 mM $(CH_3COO)_2Mg$, 5 mM CH_3COONa, and 2 mM dithiothreitol). After washing three times with transport buffer, cells were incubated at 30 °C for 30 min in the presence of energy-regenerating system (1 mM ATP, 1 mM GTP, 10 mM creatine phosphate, and 20 U/ml creatine phosphokinase), 3 μM DsRed-labeled recombinant protein, and cytoplasmic extract from 2×10^5 HeLa cells. Samples were washed three times in transport buffer, fixed on ice for 30 min with 1% formalin/transport buffer and analyzed with a Leica QFluoro system.

2.10. Immunoblotting

293T cells were co-transfected with an HA-tagged human Nup98-expressing plasmid DNA (pcDNup98) and a siRNA-expressing plasmid (siN98 or siLuc). Three days after transfection, the cells were washed twice and lysed in RIPA buffer (0.5% NP-40 in 20 mM Tris–HCl [pH 8.2], 0.15 M NaCl, 5 mM iodoacetamide, and 1 mM phenylmethylsulfonyl fluoride). After loading on SDS/PAGE, polypeptides were transferred to Immobilion Transfer Membranes (Millipore, Billerica, MA, USA), the level of Nup98 was determined using a goat anti-Nup98 polyclonal antibody (C-16), biotin-conjugated rabbit anti-goat IgG (Chemicon) and then incubated with horseradish peroxidase (HRP)-conjugated streptavidin (Zymed, San Francisco, CA, USA). The filter generated from HeLa cells infected with siRNA-expressing

HIV-1 vector as described above was also incubated with mAb414 (mainly reactive against p62), biotin-conjugated horse anti-mouse IgG (VECTOR) and HRP-conjugated streptavidin. The specific bands were detected using Western Lighting Chemiluminescence Reagent (Perkin–Elmer Life Science, Boston, MA, USA). For detection of Nup98-VSV M complex, 293T cells were co-transfected with Nup98-expressing plasmids (pcDNup98) and EGFP-fused VSV M-expressing plasmid DNA (pEGFPN3-M) or the mutant [VSV M(D)]. Two days after transfection, the cells were lysed in triple detergent lysis buffer (1% NP-40, 0.1% SDS, 0.5% sodium deoxycholate in 50 mM Tris–HCl [pH 8.0], 0.15 M NaCl, 1 μg/ml aprotinin, 1 mM phenylmethylsulfonyl fluoride), and a mouse anti-HA mAb (F-7) (Santa Cruz) was added. After incubation for 12 h at 4 °C with protein G-sepharose (Amersham), the precipitate was washed three times with triple detergent lysis buffer, and the bound proteins were eluted by 1× sample buffer (1.71% SDS in 175 mM Tris–HCl [pH 6.8], 5% glycerol, 1% 2-mercaptoethanol) at 37 °C for 30 min. The samples were loaded on SDS/PAGE and transferred to Immobilon Transfer Membranes. For detection of the Nup98, a goat anti-Nup98 polyclonal antibody (C-16) (Santa Cruz) and biotin-conjugated rabbit anti-goat IgG (Chemicon) were used. For detection of VSV M, a rabbit anti-GFP polyclonal antibody (Santa Cruz) and biotin-conjugated donkey anti-rabbit IgG (Chemicon) were used.

2.11. Statistical analysis

All data were expressed as mean ± standard deviations (S.D.). Differences between groups were examined for statistical significance using the Welch's *t*-test. A P value less than 0.05 denoted the presence of a statistically significant difference.

3. Results

3.1. Efficient nuclear import of HIV-1 cDNA in infected cells

It has been shown that HIV and HIV-based lentivirus vectors efficiently infect non-dividing cells [2,6]. To determine the integration efficiency in dividing and non-dividing cells, we prepared cell-cycle-arrested T cell culture using MT-2 cells treated with APH, an inhibitor of DNA polymerase α. Under this condition, cell-cycle was confirmed to be stopped at G1 phase from flow cytometric analysis (Fig. 1A). The same numbers of treated (arrested) or untreated (proliferating) cells were infected with the same amounts of HIV-1 vector and the arrested culture was further maintained in the presence of APH. Since in this experiment we used a single-round infection system, we could estimate the precise efficiency of reverse transcription, nuclear translocation as well as integration. Total DNA was extracted 24 h after infection and a set of real-time PCR assay was performed [16,17]. Using this assay, we were able to measure the full-length/1LTR circle, 2LTR circle and integrated forms of HIV-1 cDNA, respectively. Since the 2LTR circle and integrated forms are found only in nucleus after HIV infection [3,22], we could estimate the efficiency of nuclear entry as well as integration of HIV-1 cDNA. Fig. 1B shows that the levels of integrated, 2LTR and full-length/1LTR circle form in proliferating cultures were higher than those in arrested cultures, because the numbers of the cells were two to three times greater in proliferating culture. However, significant amounts of integrated ($4.2 \times 10^5 \pm 5.4 \times 10^4$ copies per culture) and 2LTR ($1.5 \times 10^5 \pm 1.5 \times 10^3$ copies per culture) form DNA were found in the arrested culture (Fig. 1B). Similar results were also obtained in APH-treated 293T cells (data not shown). These data correspond well with the previously reported findings of the high susceptibility of APH-treated cells to HIV-1 [3,22]. Importantly, the ratios of integrated form and 2LTR form to full-length/1LTR form were similar in the proliferating (integrated; 0.108 ± 0.024, 2LTR; 0.022 ± 0.002, full-length/1LTR; 1.0) and the arrested cultures (integrated; 0.09 ± 0.011, 2LTR; 0.031 ± 0.001, full-length/1LTR; 1.0), respectively, strongly suggesting that HIV-1 cDNA efficiently traverse NPC, depending on the active nuclear import machinery in not only non-dividing cells but also proliferating cells.

3.2. Inhibition of HIV-1 cDNA import with a Nup98-specific inhibitor

Next, to examine the specificity of our real-time PCR assay and the associated molecules in nuclear entry of HIV-1 cDNA, we prepared HIV reverse transcription-inhibited (AZT-treated), transcription-blocked (ActD-treated), or CRM1-dependent nuclear export-inhibited (LMB-treated) 293T cell cultures. As expected, AZT significantly inhibited the appearance of all forms of DNA (Fig. 2A a–c). Although dose-dependent inhibition of integration was found in ActD- or LMB-treated cultures, significant accumulation of the 2LTR form was also found (Fig. 2A f and i), suggesting that newly synthesized proteins as well as CRM1-dependent exported proteins may be required for the efficient integration but not nuclear entry of HIV-1 cDNA. To examine whether specific Nups are required for HIV infection, we used VSV M protein, a specific inhibitor protein against Nup98. It has been shown that Nup98 is involved in the nuclear import of some proteins as well as the export of RNA, and its function is specifically impaired in the presence of VSV M protein [20]. The VSV M binds a region within residues 66–515 of Nup98 that encompasses most of the FG repeats, the hRAE1/Gle2 binding site or GLEBS-like motif [23], and most of the predicted glycosylation sites of the Nups. Through these sites, Nup98 was able to interact with three

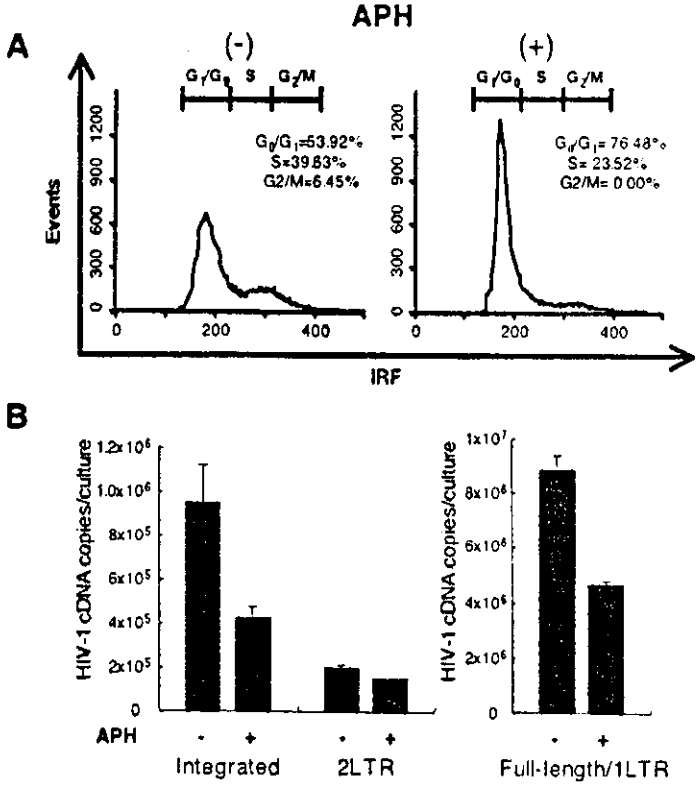

Fig. 1. Efficient nuclear entry of HIV-1 cDNA in arrested cells. (A) Cell-cycle analysis of APH-treated and -untreated cells. MT-2 cells were incubated for 24 h without (–) or with (+) APH, and then analyzed for DNA content by flow cytometry of proridium iodide-stained nuclei. Representative flow cytometry data from one of three independent experiments is shown. (B) Quantification of HIV-1 cDNA after HIV-1 vector infection in APH-treated and -untreated cells. Number of viral DNA copies per culture (baseline cell number is 2×10^5 cells) is indicated. APH-treated or -untreated MT-2 cells were infected with HIV-1 vector, and cultured without (–) or with (+) APH for another 24 h, respectively. Then, DNA was extracted and subjected to PCR assay. Results are mean ± S.D. of three independent experiments.

putative Nup98 partners: RAE1 [23], CRM1 [24], and TAP [25]. VSV M-mediated inhibition was not observed in a site-directed mutant (residue 52–54), termed VSV M(D) [20]. We used the VSV M as a specific inhibitor of the Nup98 function. An obvious impairment of integrated and 2LTR but not full-length DNA was found in only the wild-type but not the mutant VSV M(D)-transfected culture (Fig. 2B). This impairment was restored with ectopic overexpression of Nup98 (pcDNup98) (Fig. 2B, lane 5). Western blotting indicated that the overexpressed Nup98 was co-precipitated with VSV M but not VSV M(D) protein (Fig. 2C), suggesting that the overexpressed Nup98 absorbed VSV M protein, and the Nup98 function was recovered. Thus, Nup98 may have a role in nuclear import of HIV cDNA.

3.3. Depletion of Nup98 by siRNA

Next, to examine directly the involvement of Nup98 in HIV-1 cDNA nuclear import, Nup98 was depleted by the siRNA technique. After transfection with Nup98-specific siRNA-expressing plasmid, mRNA expression of Nup98 as well as Nup96, generated from the same precursor transcripts of Nup98 [26], but not other Nups such as p62, Nup107, Nup153, and Nup214, were specifically inhibited (Fig. 3A). It was also confirmed that the level of ectopic Nup98 protein expression was inhibited with the siRNA-expressing plasmid as it was lower than that in its endogenous expression (Fig. 3B). Immunofluorescence analysis using an anti-Nup98 antibody also confirmed the significant inhibition of Nup98 expression on nuclear membrane in the Nup98 siRNA-targeted HeLa cells using a siRNA-expressing lentivirus vector (Fig. 3C, upper panel). We further examined the distribution of NPC components using mAb414, an antibody known to interact with many FG-containing Nups, mainly p62 and to a less degree, Nup153, Nup214, and Nup358 but not Nup98. The Nup98 siRNA-transduced cells exhibited weak mAb414-labeling intensity at the nuclear rim and shift of labeling to the cytoplasm, probably cytoplasmic annulate lamellae (Fig. 3C, lower panel). However, the total amount of p62 (main component of NPC) was similar in both Nup98-siRNA-targeted or control cultures (Fig. 3D). A previous study using Nup98 knockout mice indicated that Nup98 is essential for rapid cell proliferation but dispensable for basal cell growth and some specific destruction of NPC component [27]. The Nup98-knockout cell was reported to have a thin nuclear envelope as well as many cytoplasmic annulate lamellae. Our Nup98-siRNA-targeted cells had similar structures. It was also reported that the mutant pores of the knockout cells were clearly impaired in in vitro transport

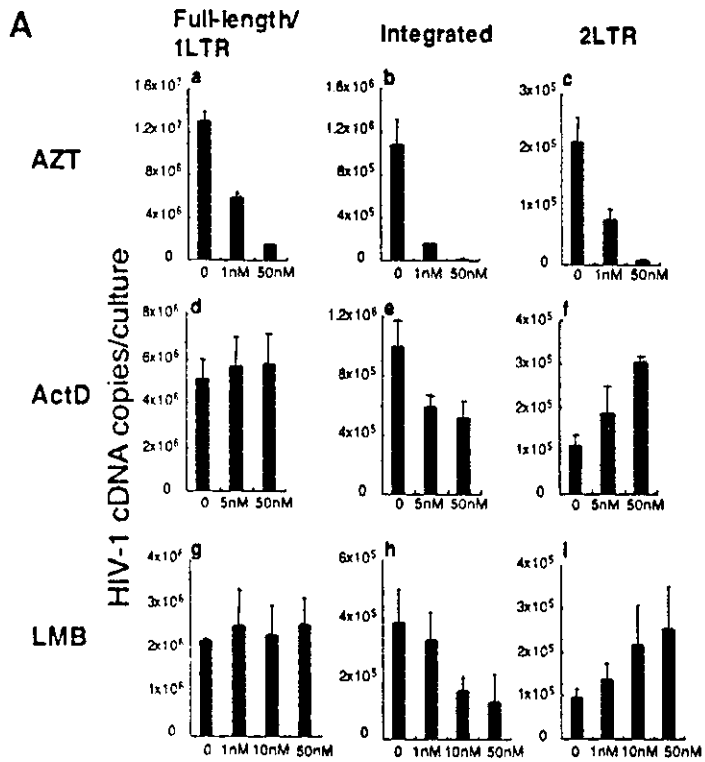

Fig. 2. Measurement of nuclear entry and integration of HIV-1 cDNA in cells treated with inhibitors. (A) Inhibition of HIV-1 cDNA appearance with chemical treatment. 293T cells were infected with HIV-1 vector at a m.o.i. of 0.5–1 and cultured in the presence of AZT, ActD, or LMB at indicated doses. HIV-1 cDNA copy numbers in AZT-treated (a, b, c), ActD-treated (d, e, f) and LMB-treated (g, h, i) cultures are indicated. Left panels (a, d, g) indicate full-length/1LTR circle, middle panels (b, e, h) indicate integrated forms, and right panels (c, f, i) indicate 2LTR circle, respectively. (B) Inhibition of nuclear entry of HIV-1 cDNA with VSV M transduction. Full-length/1LTR circle, 2LTR circle and integrated forms of HIV-1 cDNA in VSV M-transduced cultures are indicated. 293T cells were transfected with VSV M- or VSV M(D)-expressing DNA (lane 3, 4). pcDNA3.1/Zeo(+) was used as control (lane 2). The VSV M-transduced cells were also transfected together with Nup98-expressing DNA (lane 5). Then, these cells were infected with HIV-1 vector 24 h later. Total DNA was extracted 24 h after infection. Results are mean ± S.D. of three independent experiments (A and B). $^*P < 0.05$ was judged as a significant difference using Welch's t-test. (C) Binding of Nup98 to VSV M protein. Western blotting using anti-GFP antibody (whole lysate) indicates VSV M or VSV M(D) expression. Binding of ectopically expressed Nup98 to VSV M protein was shown by immunoprecipitation with anti-HA antibody (anti-HA IP) and Western blotting using anti-Nup98 or anti-GFP antibodies. Results of one representative experiment from three independent experiments are shown.

assays with nuclear localization signal (NLS) of SV40 or M9 import signal (mediated by importin α/β and importin β2, respectively), while the ability of the mutant pore to import ribosomal protein L23a (mediated by either importin β, importin β2, importin β3 or importin 7) [28] and splice some protein U1A (independent of cytosolic transport factors) was intact [27]. To examine the import ability of Nup98-siRNA-targeted pores, we performed a set of import assays. These experiments were performed in a transport buffer containing specific soluble transport receptors, an energy-regenerating system, and a DsRed-labeled protein acting as a substrate for import into the nuclei of digitonin-permeabilized cells [29]. The nuclear import with an SV40 NLS import signal was substantially lower in the Nup98-depleted cells than in control cells. In contrast, translocation of rpL23 or U1A was similar in Nup98-depleted and control cells (Fig. 2E, F). These results indicated that protein import pathways were similarly impaired in both Nup98-depleted human cells using siRNA and Nup98-knockout cells, although the level of impairment of NLS in the Nup98-depeleted cells using siRNA seems to be lower than that in knockout cells.

3.4. A role of Nup98 in HIV-1 cDNA import

Finally, Nup98-depleted cells using a siRNA-expressing plasmid DNA were infected with HIV-1 vector, and the levels of integrated, 2LTR, and full-length/1LTR forms of HIV-1 cDNA were measured. Obvious reductions of integrated and 2LTR but not full-length DNA were noted in the Nup98-depleted culture. In contrast, in culture transfected with a control siRNA-expressing DNA targeted for luciferase (si-Luc), the levels of integrated, 2LTR and full-length DNA were still high (Fig. 3G). These findings suggest that Nup98 in the NPC participates in the nuclear entry of HIV-1 cDNA.

4. Discussion

The major finding of the present study is that Nup98 has an important role in the nuclear import of HIV-1 cDNA, based on a series of experiments using an inhibitor (VSV M protein) and the siRNA technique for Nup98. The role of

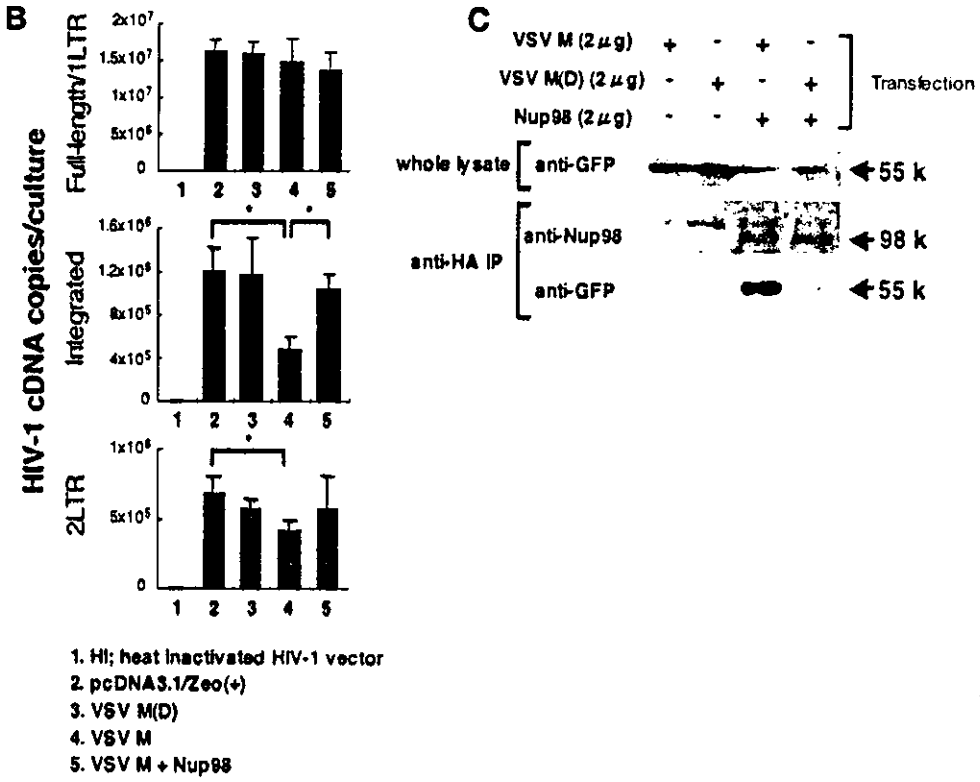

Fig. 2. *(continued)*

NPC in virus replication has been shown previously in other virus families [30]. It was reported that the import process of adenovirus type 2 DNA through NPC involves Nup214 as well as histone H1 [31]. Adenovirus capsid docks on Nup214, probably involving recruitment of importin 7/β heterodimer to the capsid, and effective disassembly at NPC activates the entry of viral DNA into nuclei [31]. Herpes simplex virus capsid docks on NPC, probably mediated by importin β alone, and undergoes a conformational shift that results in extrusion of viral DNA genome into nucleus through NPC [32]. It is possible that specific molecular events may occur at NPC during the nuclear entry of HIV-1 cDNA [15].

We recently transduced a siRNA-expressing DNA for Nup98 using lentivirus vector coexpressed H-2K^k, as described above, and at this time the culture was challenged with replication-competent EGFP-expressing HIV-1. Flow cytometric analysis indicated that numbers of HIV-1-infected cells were obviously inhibited in Nup98-siRNA-expressing T cells but not in control luciferase-specific siRNA-expressing cells. Significant reduction of HIV-1 p24^{gag} (five to sixfold) was also noted in the culture supernatant (data not shown). It was reported that Nup98 and Nup214 are required for Rev-dependent export of HIV-1 RNA [24]. Thus, inhibition of Nup98 expression by functional impairment of Nup98 by siRNA may induce inhibition of HIV-1 gene expression through inhibition of the Rev-dependent export. Some degree of the inhibitory effect of HIV-1 infection by the siRNA may be partly caused by this inhibitory effect of Rev function. But quantitative analysis of HIV-1 cDNA in single-round infection demonstrated that the inhibition of nuclear import of HIV-1 cDNA (Fig. 3G) was apart from gene expression. These findings suggest the involvement of a specific import pathway in the nuclear entry of HIV cDNA through NPC.

Most of the transport receptors identified to date are members of a large family of RanGTP binding proteins, which exhibit a limited sequence similarity to the Ran binding domain of importin β. The interaction of these receptors with Nups is regulated by small GTPase Ran. Ran is a small GTPase that cycles between a GDP-bound form (RanGDP) and a GTP-bound form (RanGTP) and plays an important role in both import and export [8]. The directional active nuclear transport is controlled by the different RanGDP and RanGTP concentration gradients within the cell. In the cytoplasm, a much higher concentration of RanGDP to RanGTP is maintained, and conversion of RanGDP to RanGTP occurs by exchanging the entire nucleotide and is catalyzed by the guanine nucleotide exchanging factor (RCC1) [33]. The exchange of the nucleotide and disassembly of importin β2 complex at a site on Nup98 was reported [13]. The VSV M-mediated inhibition of nuclear traffic is due to the inhibition of RanGDP to RanGTP conversion [13]. Therefore, in the presence of VSV M expression or inhibition of Nup98 expression should induce the disruption of the RanGDP and RanGTP concentration gradients. Our data strongly suggest